Alma Mater Studiorum - Università di Bologna

DOTTORATO DI RICERCA IN

SCIENZE E TECNOLOGIE AGRARIE, AMBIENTALI E ALIMENTARI

Ciclo 34

Settore Concorsuale: 07/E1 - CHIMICA AGRARIA, GENETICA AGRARIA E PEDOLOGIA

Settore Scientifico Disciplinare: AGR/07 - GENETICA AGRARIA

QTL MAPPING IDENTIFIES NOVEL MAJOR LOCI FOR EAR FASCIATION, EAR PROLIFICACY AND TILLERING IN MAIZE (ZEA MAYS L.)

Presentata da: Kai Li

Coordinatore Dottorato

Massimiliano Petracci

Supervisore

Silvio Salvi

Esame finale anno 2022

Index

Abstract

Maize ear fasciation originates from excessive or abnormal proliferation of the ear meristem and usually manifests as multiple-tipped ear, ear flatness and/or disordered kernel arrangement. Ear prolificacy expresses as multiple ears per node. Both traits can affect grain yield. In this study, the genetic control of the two traits was analyzed using two recombinant inbred lines (RIL) populations (B73 × Lo1016 and Lo964 × Lo1016) with Lo1016 and Lo964 as donors of ear fasciation and prolificacy, respectively. Four ear fasciation-related traits (ear fasciation, kernel distribution and ear ovality indexes and ratio of ear diameters), number of kernel rows, ear prolificacy and number of tillers were phenotyped in multi-year field experiments. Ear fasciation traits and number of kernel rows showed relatively high heritability ($h^2 > 0.5$) except ratio of ear diameters, and showed correlation. Prolificacy and tillering h^2 ranged 0.41 - 0.78 and did not correlate. QTL mapping identified four QTL for ear fasciation, on chr. 1 (two QTLs), 5 and 7, the latter two overlapping with QTLs for number of kernel rows. However, the strongest effect QTL for number of kernel rows mapped on chr. 2 independently from ear fasciation. Four and five non-overlapping QTLs were mapped for ear prolificacy and tillering, respectively. Two ear fasciation QTLs from this study, *qFas1.2* and *qFas7*, overlapped with formerly known fasciation QTLs and spanned candidate genes expressed in ear meristems namely *compact plant2* and *ramosa1*. Our study identified novel ear fasciation, ear prolificacy and tillering loci which are unexpectedly still segregating in elite maize materials, and provides foundation for genomics-assisted breeding for yield components.

1. Introduction

Fasciation is a deviational proliferation of cells and tissues eventually manifesting as widen and flattened organs, most commonly arising from indeterminate tissues of actively growing organs such as stems or inflorescences, reported in more than 107 plant families, including trees, shrubs and grasses (White, 1948; Iliev and Kitin, 2011) . Fasciation was interpreted as (i) an excrescence or fusion of organs due to deviations from normal meristematic processes or crowding of buds, or (ii) a transformation of a single growing point into a line, this sometime called 'true fasciation' (Clark *et al.*, 1993; Iliev and Kitin, 2011) .

Fasciation can originate as a consequence of natural factors artificial treatments, or by mutations (Iliev and Kitin, 2011; Ortez *et al.*, 2022) . Fasciated mutants can be of interest in plant breeding programs for their ornamental characteristics or because their abnormal development may favorably affect yield components such as fruit and/or seed size and number. This is the case for tomato cultivars where fasciation contributed to increase the number of fruit locule and fruit size (Tanksley, 2004; Iliev and Kitin, 2011) , for a mutation in mustard (*Brassica rapa*) at the *Multilocular* locus, which increases seed production (Fan *et al.*, 2014), and for maize, where it has been suggested as a potential target for increasing ear size and/or number of kernels per ear, which are important yield components (Kim *et al.*, 2022; Somssich *et al.*, 2016). The interest in the connection between fasciation and grain yield components in maize increased in the last decades as the knowledge about the molecular control of the inflorescence meristem development accumulated. Accumulating evidences indicated that while strong fasciated ear mutants do not improve productivity as they usually lead to a shorter stunted ear, weaker alleles leading to a less disturbed inflorescence meristem show more potential to improve yield (Bommert, Nagasawa, *et al.*, 2013; Je *et al.*, 2016; Kim *et al.*, 2022; Ortez *et al.*, 2022).

Size and shape of the shoot vegetative meristem or of the early generative inflorescence meristem were early recognized as the developmental foci where genetic defects could determine the production of a fasciated inflorescence (Galli and Gallavotti, 2016; Kyozuka *et al.*, 2014). One of the key regulation pathways is the CLAVATA3 (*CLV3*)-WUSCHEL (*WUS*) feedback signaling which controls stem cell proliferation and tissue and organ differentiation

(Somssich *et al.*, 2016). This mechanism is achieved based on a negative-feedback loop mainly consisting of the stem cell-promoting transcription factor, WUSCHEL, and the differentiation-promoting peptide *CLV3* that is expressed only in stem cells of the shoot apical meristem (SAM) and belongs to CLAVATA3/EMBRYOSURROUNDING REGION (ESR) CLE peptide family (Trotochaud *et al.*, 1999; Opsahl-Ferstad *et al.*, 1997). With this loop, WUS activities are firstly repressed by an extracellular protein encoded by *CLV3*, causing decline of stem cell multiplication, and correspondingly, decrease in *CLV3* production (Brand *et al.*, 2000; Schoof *et al.*, 2000). Therefore, such parallel feedback mechanism keeps the size of the organizing center, in terms of number of cells, under control (Müller *et al.*, 2006).

CLV-WUS meristem size regulatory pathway acts across plant species, including crops such as maize, rice and tomato. For example, an ortholog of *CLV3* in rice, *FLORAL ORGAN NUMBER 2* (*FON2*) (also identified and named independently as *FON4*) was found to express specifically in a few cells in the shoot apical region and is responsible for regulating floral organ number (Chu *et al.*, 2006; Suzaki *et al.*, 2004), while another *CLV3* ortholog in maize, *ZmFCP1*, is mainly expressed in leaf primordia (Rodriguez-Leal *et al.*, 2019), unlike its counterpart, *FCP1* in rice (Suzaki *et al.*, 2008) which is expressed in shoot. In *fea3* mutants in maize, SAM size showed significant decline when *ZmFCP1* peptides and *fea3* embryos showed resistance only to *ZmFCP1*, indicating *FEA3* functions as a receptor of *ZmFCP*1 (Somssich *et al.*, 2016). In contrast, *FEA2*, the *CLV2* ortholog in maize, involved more widely in regulating activities of correlated CLE peptides, including *ZmCLE7* and *ZmFCP1*, *ESR2c* (Je *et al.*, 2018), and *fea2*-null mutants have larger KRN compared with wild-type plants, as there are 30 or more irregular kernel rows in mutants (Bommert, Nagasawa, *et al.*, 2013). Similarly, a downstream effector, *COMPACT PLANT2* (*ct2*) is also able to achieve signaling transition from these distinct CLE peptides, suggesting the whole mechanism appears like the CLV-WUS pathway in *Arabidopsis* (Bommert, Nagasawa, *et al.*, 2013).

Besides these, other genes have been identified which function is not completely clear, however their mutants showed evident ear fasciation. For example, in the mutants of *UNBRANCHED3* (*UB3*), the size of the inflorescence meristem is mediated positively and kernel row number is increased, suggesting *UB3* regulates vegetative and reproductive

branching in maize (Du *et al.*, 2017). Additionally, the QTL *KERNEL ROW NUMBER4* (*KRN4*), mapped in an intergenic region on chr 4 (Liu, Du, Shen, *et al.*, 2015), nearby *UB3*, was recognized as a *cis*-regulatory element of *UB3* (Du *et al.*, 2020) *UB2*, a paralog of *UB3*, also encoding SBP-box transcription factors, plays a redundant role with *UB3* in controlling the initiation of reproductive axillary meristems and interacts physically with *KRN4* (Du *et al.*, 2020).

As already anticipated, most of these traditional mutants showed negative pleiotropy on grain yield and it has been difficult to utilize them directly in breeding. For example, fasciated ear mutants such as ramose mutants, *ra1*, *ra2* and *ra3*, usually develop shorter ears with disordered seed rows, resulting in decreased kernel number. More promising seems to be the use of some weaker alleles for the same genes, possibly in heterozygosity in F_1 hybrid combinations (Bommert, Je, *et al.*, 2013; Bommert, Nagasawa, *et al.*, 2013; Gallavotti *et al.*, 2010).

In maize, prolificacy is a general term indicating the presence of multiple ears in a plant and can be classified as three types: multi-node prolificacy (multiple ears growing at different nodes), multi-tiller prolificacy (multiple stems grow from nodes), and single-node prolificacy (multiple ears growing at the same nodes, also known as 'multi-ears' or 'bouquet ears' or 'shank ears'; (Ortez *et al.*, 2022). In this study we will specifically focus on single-node prolificacy. In single-node prolificacy, the presence of multiple ears is the result of multiple axillary meristems located on the same ear shank giving rise to additional ear inflorescences alongside the central one. Their developmental timing is assumed to be early, starting from stages V4-V6, however it can extend up to pollination (Abendroth, L.J., Elmore, R.W., Boyer, M.J., and Marlay, S.K., 2011). The presence a single major ear per plant versus multiple ears is one the major contrasting difference between currently cultivated maize and its progenitor teosinte (Stitzer and Ross-Ibarra, 2018). Because of this, domesticated maize was referred as "not prolific", while its progenitor teosinte as "prolific" (Yang *et al.*, 2019; Doebley *et al.*, 1995; Prakash *et al.*, 2019). While most of the modern maize hybrid cultivars cultivated in the high-dense stands in temperate environment develop only one ear, the potential presence of multiple ears per plant

has physiological and breeding implications. For instance, maize hybrid cultivars with some level of plasticity to develop tillers and multiple ears per plant may turn out advantageous in semi-arid regions with high inter-annual variation of summer rainfall, where they are cultivated at low plant population densities (i.e., less than 4 plants m-2) (Rotili *et al.*, 2022). More specifically Rotili et al. 2002 suggested that a multiple-ear genotype could provide higher yield when the environmental conditions would have prevented the development of tillers, in a cropping system characterized by low plant density. Another situation where ear prolificacy is considered a positive feature is in cultivars utilized for baby corn production used for human consumption. Baby corn is a type of specialty food where unfertilized maize ears are consumed in salads, soups, fried snacks etc. Major baby corn markets exist in United Kingdom, United States of America, Malaysia, Taiwan, Japan and Australia, which mainly import baby corn from international markets especially Thailand (Prakash *et al.*, 2019).

The genetic control of multiple ears per plant is complex, as it involves at least three different mechanisms as introduced above. However, only a few studies have so far addressed the genetic control of this trait. A major QTL for single-node prolificacy, *prol1.1,* was mapped on chr. 1 in a maize-teosinte BC_2S_3 population, at a chromosomal location that has previously been shown to influence domestication traits. The authors identified *prol1.1* ‘‘causative region’’ as a transposon insertion upstream of the *grassy tillers1* (*gt1*) gene, which encodes a homeodomain leucine zipper transcription factor (Wills *et al.*, 2013). Prakash et al (2021) took advantage of a multi-node prolific maize inbred characterized by five to nine ears per plant to cross two non-prolific inbred. Results showed that a sizeable portion of prolificacy phenotypic variation (c. 30%) was controlled by a major locus in bin 8.05 between umc2199 and bnlg1031. Multi-node prolificacy was also addressed in a large study involving two experimental RIL populations and one germplasm collection leading to the identification of several QTL on all chromosomes (Wang *et al.*, 2021).

It should be noted that ear and tillers both originate from axillary buds developing into shorter or longer shoots, therefore they are expected to share an important portion of genes and regulatory mechanisms. This was indeed confirmed by the identification and cloning of genes such as *BARREN STALK1* (*BA1*), encoding a bHLH transcription factor orthologous to rice

LAX PANICLE1 (*LAX1*) (Gallavotti et al. 2004). ba1 mutants fail to initiate all vegetative and reproductive axillary meristems. *BA1* levels are under the control of *BARREN STALK FASTIGIATE1* (*BAF1*), a transcriptional regulator with an AT-hook DNA binding motif (Gallavotti et al. 2011). Mutant *baf1* plants fail to initiate axillary buds that are fated to become lateral ear shoots; as a result, *baf1* mutants are earless (Gallavotti et al. 2011).

Conventional breeding methods applied to maize and other crops basically depend on phenotypic selection in order to identify filial individuals to be deployed as new cultivars. In maize, these progenies should also be characterized by heterosis (or even heterobeltiosis, namely the superiority of the F1 hybrid to the best parent). The process is extremely complex, and time and resource expensive. In order to overcome limitations in traditional breeding, marker assisted selection (MAS) was introduced as an efficient supplementary method, in which differences of genetic sectors involved in agronomic phenotypes under studying are able to be recognized by molecular markers. By developing an array of molecular markers and genetic maps, and building correlations between genotypes and phenotypes, it is more likely to map those quantitative trait loci (QTL) and functional genes, thus accelerating the breeding process. With availability of cheaper sequencing technologies, utilization of molecular markers appears a gradual shift from simple sequence repeats (SSRs) to single nucleotide polymorphisms (SNPs) in mapping studies (Choudhary *et al.*, 2019). Additionally, a more cutting-edge technology in maize breeding is the application of CRISPR-CAS9 system for gene editing. This system is similar to scissors, cutting the DNA, or genes at a particular spot, usually called as the binding site, resulting in elimination, adding, or overexpression of the target genes. (Agarwal *et al.*, 2018)

Besides adequate molecular markers, mapping populations with sophisticated design are also required in order to verify genetic sectors with phenotypic variation, thus linking polymorphism with traits. Types of mapping population which were applied ever and are utilized presently include second filial generation (F_2), backcross (BC), recombinant inbred lines (RILs), double haploids (DHs), and near isogenic lines (NILs), in which F_2 and BC carry the most convenient experimental populations designed for self-pollination crops, deriving from selfing F_1 hybrids which are developed by crossing of two parent lines and from crossing

F_1 lines with one of the parents respectively, on the base of which two three other populations are allowed for creating. For example, recombinant inbred lines originate from inbreeding from individual F_2 plants after 7-8 generations, which ensures that a series of offspring lines are homozygous and each individual carries a unique recombination segment from the two initial parents, and near isogenic lines are developed by generational backcross selection by at least 6 times and then selfing BC_7 by two generations, aiming to screen lines carrying homozygous sectors for the target genes (Glover *et al.*, 2004). Doubled haploid (DH) populations could be produced through both *in vivo* and *in vitro* systems, such as by parthenogenesis, pseudogamy or chromosome elimination after extensive crossing in order to nurture haploid embryos, in spite of restricted application only in species enabling to culture tissues, including crop (barley, maize, rice etc.) and tree species (oak etc.) (Maluszynski *et al.*, 2014).

According to Xu (Xu, 2012), several classification standards could be applied in order to describe their properties genetically based on genetic constitution, maintenance and genetic background of progeny populations. According to the first classification, mapping populations constructed could be divided into four types: homogeneous populations with homozygous individuals, including individuals originating from an inbred developed by open pollination; homogeneous populations with heterozygous individuals, such as F1 plants crossed by two homogeneous individuals in an open-pollinated population; Heterogenous populations with homozygous individuals, such as RIL populations; Heterogenous populations with heterozygous individuals, such as F2 populations. According to the second classification, they could be separated into two types based on whether the genetic constitution of a population could be maintained after selfing by one or more generations: Temporary populations, including F2, BC populations since segments of their chromosome would create recombination as selfing or inbreeding, resulting in utilization only once; Permanent populations, such as RIL, NIL populations, because these types of populations consist of a set of pure-breeding lines, which means that they have almost identical genotypes across the whole genome except minor alleles distributed randomly. Besides, it appears extremely simple to divide based on genetic background by which these populations could be separated from those which have nearly isogenic background and those which have heterogenous backgrounds.

Additionally, in the past decade years, more complex mapping populations have been proposed and applied in both association and linkage mapping practically. Multi-founder populations recognized as a second-generation mapping approach, different from bi-parental populations which are symbolled with small scales and underpowered, are initially designed for mapping multiple QTL for a series of phenotypes despite more expending on labor and time required when creating such populations, in which Nested-association-mapping (NAM) populations, Multiparent advanced generation intercross (MAGIC) populations are the two widely applied.

Nested-association-mapping (NAM) population, firstly proposed by Yu (Yu *et al.*, 2008) in 2008 in order to proceed outcrossing in maize and firstly published by McMullen (McMullen *et al.*, 2009) in 2009 consisting of 25 maize inbred lines crossing with a common recurrent parent B73 and developing 5,000 RILs finally, enables combination of advantages of linkage mapping and association mapping parallelly: substantial scales of populations provide enough power to map loci in the linkage analysis with less need for high density markers, while the utilization of more rapidly decaying LD across the multiple founders improves precision in the association mapping (Yu *et al.*, 2008). However, NAM populations face a major limitation: no novel haplotype would be generated when only one common parent is used. This defect could be remedied in Multiparent advanced generation intercross (MAGIC) populations, another mapping approach when multi-parents are used. MAGIC is developed by intercrossing multiple founders (typically eight) with multiple rounds before construction of offspring lines for genetic mapping, and 28 possible F1 (2-way) crosses and 210 possible four-way crosses among unrelated F1s and another 315 possible ways of creating the eight-way crossed exist (Mackay *et al.*, 2014). This type of populations has been utilized involve in many important crops, including rice (Bandillo *et al.*, 2013; Meng *et al.*, 2016), wheat (Huang *et al.*, 2012; Mackay *et al.*, 2014), maize (McMullen *et al.*, 2009), and tomato (Pascual *et al.*, 2015). MAGIC populations bear representative beneficial factors compared with bi-parental and/or identical association-mapping populations: Firstly, more abundant genetic variations exist across the whole genome when involving in multiple parent lines; Secondly, frequencies of alleles are more balanced due to the equal contribution of founder to the whole population; Thirdly,

recombination events are proximately densely and evenly distributed, thus providing substantial resolution for constructing genetic maps and isolating target genes.

In this study, we investigated the genetic control of ear fasciation and ear prolificacy and the connection of these traits with kernel row number and tillering, respectively. We addressed this by exploiting two RIL populations, B73 × Lo1016 and Lo964 × Lo 1016, which are all elite maize dent lines. Lo1016 is an inbred line characterized by mild ear fasciation, while Lo964 is characterized by multiple-ear at single node.

2. MATERIALS AND METHODS

Plant materials and marker genotyping

Two recombinant inbred line (RIL) populations were developed at DISTAL, University of Bologna, as follow. The Italian-origin inbred line Lo1016 was crossed with B73 and with Lo964, a second inbred line originated from Italy to create two F_1s. Both Lo964 and Lo1016 were bred at the Bergamo breeding station (Italy), shown to be relatively related based on molecular marker analysis, and classified to the BSSS = Iowa Stiff Stalk Synthetic heterotic group (Alessia Losa, Hans Hartings, Alberto Verderio, Mario Motto, 2011). B73 is the maize inbred line of reference (Schnable *et al.*, 2009). We proceeded by single seed descent method until F7. Since the F7 stage, seeds from each line were obtained and multiplied following standard procedures. The RIL B73 × Lo1016 (B×L) and Lo964 × Lo1016 (L×L) eventually included 97 and 68 recombinant inbred lines, respectively. We will refer to Joint Population (JP) as the assembly of whole set of 165 (97 + 68) RIL lines.

Field experiment and phenotypic data collection

Field trials for the phenotypic analysis of ear fasciation and ear prolificacy, including the two RIL populations and parental lines were carried out in Cadriano, near Bologna, Italy (44°33'02.5"N, 11°24'43.9"E) in 2017 and in Monselice, near Padua, Italy (45°12'42.4"N,

11°45'14.8"E) in 2018 and 2019. Field experiments were organized as randomized complete block design with two replicates (one rep = one plot with 10 plants per RIL line). Plots for each of the three parental lines were included in the experiment. Plot length was 2.5 m, distance between rows was 0.8 m and between plants was 0.17 m. Plots were overplanted by hand and thinned at the V7 growth stage to one plant per hill equivalent to ten plants per plot, and with an overall investment of 10 plants per square meter. The field management followed standard agronomic practices of the area.

Phenotyping for ear fasciation was addressed by collecting four traits, namely 'ear ovality' (OVA, defined after visual inspection of elliptic/flatness degree of cob cross-section, from 0 to 10, corresponding from perfect circle to extremely elliptic/flat cob cross sections, respectively; higher values indicated strong fasciation); 'kernel row disorder' (DIS, defined as a visual score for from 0 to 10, corresponding from perfectly linearly arranged kernels on ears to highly disordered arrangement, respectively; higher values indicated strong fasciation); 'ear diameter ratio' (DIA, defined as ratio of minimum diameter divided by maximum diameter, where the two diameters were measured mutually perpendicularly by a vernier caliper at the middle of maize ear; lower values corresponded to strong fasciation); 'ear fasciation' (FAS, a visual score for ear fasciation scaled from 0 to 3, where 3 indicated a strongly fasciated ear). Visual scores per ear were given by three persons independently, and mean values were utilized as entries for subsequent analysis. Number of kernel rows (KRN) was collected by counting the number of kernel rows at mid ear position, on the same ears subjected to phenotyping for fasciation. Plant architecture traits collected were number of tillers per plants (TIL) and proportion of plants per plot showing prolificacy (i.e. >1 ear at the top ear node, PROL).

Raw phenotypic data for all traits were modified by using the model Best Linear Unbiased Estimator (BLUES) in the R package "tidyverse"(Wickham *et al.*, 2019). BLUES values were utilized for biometric summary, and correlation and QTL analysis. Correlation analysis was carried out by Spearman method (Wickham *et al.*, 2019) (although we will use the common letter '*r*' instead of the more appropriated '*rho'* for clarity in text) which is less sensitive to deviation from normal distributions. All trait phenotypic distributions were normal or close to normality with the exception of TIL and PROL. For these traits, original distributions

resembled Poisson distribution (Fig. 2 and supp. Fig 1 and 2). While we used original data for visualization, we operated a square root transformation as suggested in (Sokal and Rohlf, 2012) for the datasets to be used for QTL mapping.

SNP genotyping, construction of linkage map and QTL mapping

B×L and L×L were genotyped using a high density 15K SNP array (Rousselle *et al.*, 2015) using a commercial service. Genomic DNA was prepared following standard protocols by a DNA extraction kit (NucleoSpin Plant II, Macherey Nagel, Duren, Germany) based on the manufacturer's protocol. Marker alleles from Lo1016 were coded as 0, alleles from Lo964 and B73 were coded as 2, and missing values were coded as -1. Linkage map construction was obtained using Icimapping (Meng *et al.*, 2015), by first removing redundant markers using the procedure "BIN", and then building linkage maps using "MAP". Three linkage maps were constructed, one for each biparental cross RIL population, and one as joint population linkage map. For "BIN" function, markers whose missing rate is higher than 50% and distortion rate is higher than 0.01 were deleted. For "MAP" function, the algorithm nnTwoOpt and SARF (sum of adjacent recombination fractions) for rippling were applied, and the window size was specified as 9.

QTL mapping was carried by QTL Icimapping, with the function 'BIP' for RIL population and 'NAM' for the two populations analyzed as a whole (Joint Population, JP). The scanning step was set as 0.1 cM in NAM and 1 cM in BIP respectively. Probability of stepwise regression was set to 0.0001. All QTL results were produced using composite interval mapping (ICIM). The LOD threshold for declaring QTL significance was set as 3.3, 3.6 and 4.6, for B×L, L×L and JP, respectively, after permutation test ($P \leq 0.05$, 1,000 permutation). QTL additive effects were always computed considering the formula 2a = (mean homozygous B73 – mean homozygous Lo1016) or 2a = (mean homozygous Lo964 – mean homozygous Lo1016), for the two RIL populations.

Screening candidate genes and variant calling

QTL confidence intervals from this study were projected on B73 reference genome Zm-B73-REFERENCE-NAM-5.0 (Hufford *et al.*, 2021) and included gene models were considered for further investigations. Whole genome sequencing of the two lines Lo964 and Lo1016 was carried out with Illumina HiSeq PE150 at 20× of coverage. Reads were aligned to the B73v5 using BWA v.7.17 (Li and Durbin, 2009). Variants were called with BCFtools v. 1.10.2 (Li, 2011) and were filtered for a minimum reads depth of 10×, PHRED quality > 40 and a minimum DV/AD ratio of 0.8, where DP is the coverage depth at the variant position and AD is the allelic depth of the alternate allele. Variant effects were predicted with SNPEff v.3.0.7 (Cingolani *et al.*, 2012) and among variants in the gene space, only high or moderate effects were considered. Additionally, alleles sequences of candidate genes were extracted for LO964 and LO1016 from their whole .vcf files and the fasta sequences were obtained with the command bcftools consensus. The 25 NAM founder sequences were downloaded from MaizeGDB (Portwood *et al.*, 2019). The fasta sequences were aligned using MUSCLE(Edgar, 2004) from MEGAX(Kumar *et al.*, 2018). The coding sequences were obtained starting from the genomic sequence and the Zm-B73-REFERENCE-NAM-5.0_Zm00001eb.1.gff3 annotation file downloaded from MaizeGDB, using GFFRead (Pertea and Pertea, 2020). The alignment images were elaborated with Jalview (Waterhouse *et al.*, 2009). Finally, a review of published QTL and genes in maize was carried out by searching major bibliographic databases using ‘ear fasciation’, ‘prolificacy’ or ‘tillering’ terms as keywords, and information on QTL and genes physical position, bin, and type of mapping population was collected.

3. RESULTS

Trait biometrics, heritability and phenotypic correlations

Preliminary observations that Lo1016 is characterized by ear fasciation and Lo964 by ear prolificacy were confirmed in this experiment (Fig. 1 and Table 1). Lo1016 showed extreme values for ear fasciation indexes as compared to Lo964 and B73 except DIS (Tab. 1. $P < 0.01$

for all comparisons for DIA, FAS and OVA, Tukey's test). Alongside, Lo1016 also showed the highest KRN (19.75 *vs* 16.33 or 14.54, for B73 or Lo964, respectively, $P < 0.01$). Lo964 showed the highest ear prolificacy (2.75 *vs* 0.0 or 0.25, for B73 or Lo1016, respectively, $P < 0.01$). In addition, Lo1016 was the only parental line developing tillers. Values for additional plant architecture traits recorded in this study are reported in Table 1.

Broad sense heritability (h^2) for ear-fasciation traits ranged from 0.13 for DIA in L×L to 0.95 for FAS in B×L. Ear prolificacy and TIL h^2 were relatively high (ranged between 0.41 and 0.78. Table 1).

Positive transgressive segregation was observed for TIL only, with some RIL lines belonging to both populations that showed >5 tillers per plant as compared to 1.5 tillers per plant in Lo1016 (high tillering parent). Negative transgressive segregation was observed for KRN, with RIL lines from L×L showing as few as 12.7 kernel rows per ear as compared to 14.5 or 19.7 kernel rows per ear recorded for Lo964 or Lo1016. Negative transgressive segregation was also observed for DIS in both RIL populations.

All four ear-fasciation-related traits resulted highly correlated, ranging from |0.48| to |0.68| ($P < 0.001$, Fig. 2. Supp. Fig. 1, 2), with DIA negatively correlated as expected (ie. the smaller DIA score, the higher ear fasciation). Additionally, these four traits correlated with KRN, with ear fasciation index being the most correlated ($r = 0.51$) and DIA the least ($r = -0.30$. All P <0.001. Fig. 2), again with DIA as the only trait showing negative correlation. Overall, these correlation results suggested that variation for KRN and ear fasciation could partially be due to the same loci. Interestingly, ear fasciation traits showed no correlation with ear prolificacy or tillering (Fig. 2).

Linkage maps

The three linkage maps, namely B×L , L×L and JP included 1,186, 984 and 1,303 markers, and covered 1,819.52 cM, 2,504.5 cM and 1,661.0 cM, respectively (Table 2 and Supplementary Figure 2). The different linkage maps covered well the maize genome with the unavoidable exception of those regions characterized by lack of markers polymorphism due to

identity-by-decent between lines. In B×L, those regions were identified as the middle part of chr 1 between PZE-101130395 (168,493,734) and PZE-101137700 (180,295,042), accounting for 3.8% of the whole chromosome, and the upper and lower parts of chr 3, for a total of 88.7 Mb (37.6% of the chr. 3 genome). In L×L , almost the whole chr 3 resulted monomorphic and thus uninformative for QTL mapping. Additionally, deficits of polymorphic markers resulted in long intervals between markers on the upper parts of chr 4 and 7, accounting for 4.9% and 7.0% for each corresponding chromosome respectively. Overall, the 87.7% and 75.7% of the maize map was sufficiently covered by molecular markers in B×L and L×L respectively.

QTL results

Four ear-fasciation QTL were identified and ear-fasciation alleles were always contributed by Lo1016

In the following, QTL for different ear fasciation-related traits (ear diameters rate, kernel disorder, ear fasciation index, ear ovality) will be considered as the same QTL whenever their supporting intervals overlap. Four QTL for ear fasciation traits were mapped (on chr 1, *qFas1.1* and *qFas1.2*; chr 5, *qFas5;* and chr 7, *qFas7*. Table 2). *qFas1.1* and *qFas1.2* were detected for ear diameters rate and fasciation index, respectively, and mapped nearby on chr 1 (bins 1.01/1.02) within two narrow supporting intervals of <2 Mb, and both segregated within B×L only. *qFas5* was mapped on bin 5.07 for fasciation index and ear ovality and appeared to segregate mainly in L×L. *qFas7* was mapped on bin 7.02 and shown to affect ear fasciation index, ear ovality and kernel disorder in both B×L and L×L. Notably, for all *qFas* QTL, the fasciation-increasing allele was provided by Lo1016, ie. the parental line showing ear fasciation (Fig. 1), as indicated by the direction of QTL effects ($2a > 0$ in *qFas1.1*, for ear diameter rate where lower values corresponded to strong fasciation, whereas $2a < 0$ for *qFas1.2*, *qFas5* and *qFas7*. Table 2).

QTLs for Number of kernel rows (KRN) partially overlapped to ear fasciation QTLs

Five QTLs for KRN were mapped. The QTL with the strongest effect, *qKRN2*, was mapped on bin 2.02 in a < 2 Mb-supporting interval and explained 13% or 23% (JP or L×L, respectively) of phenotypic variation with a genetic effect 2a = 0.69 or 0.87 kernel rows, in JP or L×L , respectively ('+' allele from Lo964). *qKRN5* was mapped on bin 5.07, controlled 10% of phenotypic variance and showed an effect of 2a = − 0.57 kernel rows ('+' allele contributed by Lo1016). Two KRN QTLs, *qKRN7.1* and *qKRN7.2*, mapped on bin 7.02 and 7.03, respectively, and had similar genetic effect (2a = −0.62 and −0.65 kernel rows, '+' allele by Lo1016). *qKRN8* mapped on bin 8.02, with a genetic effect of 2a = −0.79 in L×L ('+' allele by Lo1016). Notably, all KRN QTLs segregated in L×L while none in B×L. *qKRN2* was the only KRN QTL with the '+' allele contributed by Lo964, while Lo1016 contributed the '+' allele in the other four KRN QTLs (Table 2). Quite interestingly, two out of five KRN QTLs overlapped with ear fasciation QTL. Specifically, *qKRN5* overlapped with *qFas5* on bin 5.05 and *qKRN7.1* with *qFas7* on bin 7.02. At both chromosome regions, the ear fasciation-increasing allele (provided by Lo1016) also increased kernel row number (Table 2), supporting the hypothesis of a functional association due to the presence of causative gene(s) affecting both ear fasciation and number of kernel rows, and in line with the observed positive correlation between the two traits (Fig. 2).

Ear prolificacy is under simple genetic control in B×L and L×L cross populations, independently from tillering

Ear prolificacy was shown to be under a relatively simple genetic control, with four QTL identified (*qProl1, qProl2, qProl4* and *qProl9.* Table 2) and the highest LOD and PVE values were provided by *qProl2* (LOD = 6.34) and *qProl9* (PVE = 16.72) respectively. More specifically, *qProl1* and *qProl4* were detected in L×L only, *qProl2* was mapped in JP, *qProl9* was mapped in B×L only. At *qProl1, qProl2* and *qProl4*, the high ear prolificacy parent Lo964

contributed the '+' QTL allele. Both *qProl1* and *qProl2* were mapped in narrow physical supporting intervals (0.8 Mb and 3.3 Mb, respectively).

Tillering variation was also shown to be under a relatively simple genetic control, with four QTL mapped. The two strongest QTLs in terms of genetic effect, *qTil1* and *qTil2*, mapped on bin 1.05 and 2.01, controlled 12-13% of phenotypic variance (in JP) with a genetic effect of 2a = 0.6 tillers per plant (in JP). The '+' allele was contributed by Lo1016 for *qTil1, qTil4 and qTil9,* in both B×L and L×L, however, B73 contributed a (+) tillering allele at *qTil2*. No overlap was found between prolificacy and tillering QTL.

Ear fasciation and KRN QTLs on chr 1, chr 5 and chr 7 overlap with QTLs from former studies

We additionally investigated overlaps of ear fasciation and kernel row number QTL between our and other studies by producing QTL consensus maps obtained by projecting QTL on the same reference map (Figure 4, Supp Table 4). On the same consensus map major candidate genes were also projected. This analysis showed that *big grain1 homolog1* (*bgh1*) (Simmons *et al.*, 2020) and *compact plant2* (*ct2*) (Bommert, Je, *et al.*, 2013) two cloned genes affecting proliferation of ear primordium were positioned in the interval of *qFas1.2*. Interestingly, QTLs for cob flatness and KRN (*qCF1* and *qKRN1a*) were mapped at this region too by Mei et al (Mei *et al.*, 2021) (Figure 4). On chr 5, *qFas5* and *qKRN5* from our study overlapped with a KRN QTL (*qKRN5-4*) identified by Liu et al (Liu, Du, Huo, *et al.*, 2015). The higher level of overlapping with QTLs and genes from former studies was observed for our QTLs *qFas7 – qKRN7.1* on bin chr 7.02. At this position, overlaps were identified with fasciation QTLs from different independent studies such as *qCF7* and *qEF7* by Mei et al (2020) and *fa_c1* by Mendes et al (2015). Additionally, this ear fasciation locus overlapped with several KRN QTLs from different studies: Ear row number QTL from seven NAM crosses (Brown *et al.*, 2011); *qKRN7* (Mei *et al.*, 2021) , *EB7.1* (Chen *et al.*, 2019a); *qKRN7.1*, this study. Genes known to be involved in early ear development and/or expressed at the same stage

and included within the *qFas7/qKRN7.1* QTL supporting intervals are *ramosa1* (*ra1*) (Dempewolf, 2010) (further details below).

As far as ear prolificacy is concerned, a QTL consensus map has seen an obvious overlapped region between *qProl4* (4:148,677,638..181,859,161) and *prol4.1* (4:161,087,836.. 169,167,836) from Wills (Wills *et al.*, 2013) (Figure 4, Supp Table 5), both of which carry relatively high LOD values (6.22 and 6.48, respectively), indicating that it is worthy focusing efforts on fine-mapping of this region. Additionally, it should be mentioned that *qProl1* mapped in the proximity (2 Mb from the QTL mapped in Liu et al. 2019) of three ear prolificacy QTLs formerly identified in other studies (Wills *et al.*, 2013; Chen *et al.*, 2019b; Liu *et al.*, 2019) at chr 1, bin 1.01 (Figure 4, Supp Table 5), thus this chromosome region could be considered a potential single locus responsible for controlling ear prolificacy variation across maize germplasm.

Meristem genes *Compact plant2* (*ct2*), *Ramosa1* (*ra1*) co-map with QTL for ear fasciation *qFas1.2* and *qFas7*, and *Barren inflorescence 1 (bif1)* comaps with *qKRN8*.

In order to search for candidate genes of ear fasciation QTLs identified in this study, we extracted all gene models included in the QTLs supporting intervals present in B73 v4 (www.maizegdb.org) along with gene expression information in meristem and ear primordium. Alongside, a list of 42 genes involved in development and/or proliferation of ear meristem was collected by meta-analysis (Supp Table 2), thus a series of cloned genes positioned in QTL of this study being listed in Supp Tab 3, such as *compact plant2* (*ct2*) and *big grain1 homolog1* (*bgh1*) within *qFas1.2*, and *ramosa1* (*ra1*) with *qFas7*.

For instance, at *qFas1.2* (chr 1, 16.0 - 18.0 Mb), *compact plant2* (*ct2*) and *big grain1 homolog1* (*bgh1*) at chr 1, 16.7 Mb were identified as candidate genes, and at *qFas7*/*qKRN7.1* (chr 7, 110.2 - 123.9 Mb), *ramosa1* (*ra1*) chr 7, 113.6 Mb, was identified as a potential target gene which might be involved in inflorescence. Additionally, at qKRN8 (chr 8, 18.8 – 20.2 Mb), we also identified *barren inflorescence1* (*bif1*), chr 8, 18.9 Mb, as a candidate KRN-gene.

As far as tillering is concerned, two candidate genes *crr1* (cytokinin response regulator1, gene model Zm00001d001865) and *arftf3* (ARF-transcription factor 3, gene model Zm00001d001879) were identified within the supporting interval of *qTil2*, on chr. 2.

Investigation of nucleotide and aminoacid sequence variation at candidate genes for ear fasciation and number of kernel rows QTLs

In order to start testing some of the candidate genes for ear fasciation and number of kernel rows, genomic sequences of B73, Lo964 and Lo1016 were recovered and compared for all the genes listed in Supp Table 2-3. At *qKRN7.1/qFas7*, we investigated the nucleotide and aminoacid difference at *ra1* (*ramosa1*). In this case, the QTL was identified in both B×L and L×L so we searched for sequence variants between B73 and Lo1016 and between Lo964 and Lo1016. However, sequence alignment showed that no difference existed between the three lines (Supp Table 3 and Supp Figure 8). Still, it might be premature to exclude possibilities that the expression levels of *ra1* have been regulated by underlying transcription factors, thus KRN being altered. Therefore, RT-PCR of this gene could be included in future studies as well.

Another KRN-influenced gene, *ct2* was found as candidate at *qFas1.2* which segregated within B×L and not in L×L. However, no sequence differences were observed between B73 and Lo1016 (while a few amino acid substitutions are predicted between Lo964 and Lo1016. See Supp Table 3 and Supp Figure 7). The same observations hold for *bgh1* a second possible candidate gene at *qFas1.2* (Supp Table 3, Supp Figure 6). Such results do not rule out *ct2* and *bgh1* as possible candidate genes at *qFas1.2*, however, their effects on ear fasciation could be due to difference in gene expression between alleles. The differences in gene expression are not currently captured by our study and they will be addressed in a future study.

Concerning *crr1*, it was identified at *qTil2* which segregated mainly with B×L, which was in accordance with sequencing results between B73 and Lo1016 where allele substitutions have been observed, as well as aminanoacid (Supp Table 3 and Supp Figure 10). Considering this correspondence, it seems deserved to arrange fine-mapping and further analysis of gene expression.

4. DISCUSSION

The inflorescence meristem originating at leaf nodes on the maize main stem is responsible for ear formation and has been recognized to play a key role in determining yield components such as number of kernels and number of kernel rows (Otegui and Bonhomme, 1998). Recently, experimental evidences accumulated suggesting that genes originally known as mutants causing fasciated ears participate to determine the number of kernel rows on the ear and therefore could impact grain yield. Indeed, mild mutations at these genes can cause modifications of the inflorescence meristem leading either to larger meristems and/or to multiple ear growing tips which in turn produce additional kernel rows (Je *et al.*, 2016; Kim *et al.*, 2022; Somssich *et al.*, 2016). However, the underlying genetic mechanisms and regulatory networks controlling the meristem size and the emergence of additional meristematic growing centers within a meristem are only partially known and therefore the exploitation of these mechanisms for plant breeding remains challenging. Therefore, the serendipitous observation of an obvious ear fasciation phenotype in the elite maize line Lo1016 (Fig. 1A) prompted us to investigate its genetic control in order to contribute useful information on the molecular genetic mechanism leading to ear fasciation and affecting an important grain yield component. A similar rationale – the observation that Lo964 is characterized by high ear prolificacy at single node (Fig. 1B) prompted us to address the genetic basis this trait.

We phenotyped ear fasciation using four approaches, namely the rate between the minor and the major cob diameters and ear ovality (these two representing cob flatness), kernel row disorder index, and an overall fasciation index, in order to capture the two different ways ear fasciation manifests, namely cob flatness and kernel disorder, as shown previously by other authors (Kim *et al.*, 2022; Mendes-Moreira *et al.*, 2015). Confirming other authors' observations, cob flatness traits and kernel row disorder correlated, and correlated with fasciation visual index. Additionally, cob flatness and kernel disorder QTL showed some level of overlap, confirming that ear fasciation manifests both as cob flatness and/or kernel row disorder. However, both the imperfect correlation between such traits (eg. r = 0.67 between

OVA and DIS) and the presence of unique QTLs for single ear-fasciation related traits (eg. *qFas1.1*, determined by ear diameters rate collected using caliper on cobs) indicated that each fasciation-related trait is a complex quantitative trait with hidden components that should not simply be expected to derive from a pleiotropic effect of a common genetic cause. In other words, at least a few genes affected kernel disorder while did not affect cob flatness, and viceversa. The presence of QTL specific for single components of ear fasciation was already observed in (Mendes-Moreira *et al.*, 2015).

Additionally, our study shed light on the relationship between ear fasciation and KRN. Confirming former studies (Je *et al.*, 2016; Kim *et al.*, 2022; Somssich *et al.*, 2016), ear fasciation positively correlated with KRN ($r = 0.51$, $P < 0.01$), and ear fasciation and KRN QTLs showed overlaps. Specifically, two out of four ear fasciation QTLs overlapped with two out of five KRN QTLs. Furthermore, at the overlapping loci, namely *qFas5-qKRN5* and *qFas7-qKRN7.1*, the direction of genetic effects for the two traits agreed with a functional positive action of ear fasciation on the number of kernel rows, as previously hypothesized or shown. A further note of interest is that at both *qFas5-qKRN5* and *qFas7-qKRN7.1* the fasciation/KRN increasing allele was provided by Lo1016, and the effect of the Lo1016 alleles at the two QTLs was detected in both B×L and L×L . In other words, at *qFas5-qKRN5* and *qFas7-qKRN7.1*, Lo1016 carries alleles increasing both ear fasciation index and kernel row number, and such positive effect of the Lo1016 allele was detected 'across' genetic backgrounds (ie. when compared with B73 and when compared with Lo964). However, the effect on KRN was detected in the L×L background only, likely because the KRN mean value in the L×L genetic background was lower than that in B×L (15.97 and 17.40 kernel rows per ear, respectively. Table 1). Indeed, in a high KRN context such as the B×L cross, any KRN -increasing allele such as the ones from Lo1016 would likely contribute just marginally to KRN increase. In L×L, the genetic effect at both QTLs for KRN was similarly estimated to be 2a = approx. 0.6 rows per locus (0.57 at *qKRN5* and 0.62 at *qKRN7.1*), equivalent to approx. 4% (0.6/16.5 rows per ear) of the average trait value in these populations (Table 1). Homozygous Lo1016 allele substitutions at both loci are therefore expected to add approx. one row per ear, therefore contributing to c. 6% (1/16.5 rows) of grain yield. While this estimate should be considered

with great caution, this notwithstanding this increase would correspond to a rather important portion of grain yield per hectare, therefore it should be considered in plant breeding programs especially when based on marker assisted selection which could target and utilize specific alleles and/or haplotypes.

A partial pleiotropy-based connection between ear fasciation and KRN (ie. genes promoting ear fasciation will eventually affect KRN) was already observed in former studies and is supported by our QTL consensus map (Fig. 4A). For example, Liu et al (Liu, Du, Huo, *et al.*, 2015) found a KRN-QTL, *qKRN5-4* between *umc1971* and *umc1071* affecting kernel row number, and mapping nearby our *qFAS5*. Additionally, (Chen *et al.*, 2019a) mapped a QTL named *KRN7.1* ranging from 21.5 Mb to 123.7 Mb on chromosome 7 in a NAM population, thereby covering the clustering region grouped by *FAS7* and *DIS7.1*. The same locus was also identified by (Brown *et al.*, 2011) in which two ear row number (ERN) QTL appear to overlap with *qFas7-qKRN7.1* identified in our study. Another example is the relationship between the large effect QTL *KRN4*, on chr 4, with the ear fasciation-like phenotypes caused by mutations in the *UNBRANCHED3* (*UB3*) gene, which negatively regulates maize kernel row number by producing abnormally shaped ears (Liu, Du, Shen, *et al.*, 2015; Du *et al.*, 2020). *KRN4* was eventually shown to be an *UB3* long-range cis regulatory element positioned ca. 60 kb downstream of *UB3* and the presence of different *KRN4* alleles in near isogenic lines results in different levels of *UB3* expression (Du *et al.*, 2020).

We also detected loci affecting the number of kernel rows independently from ear fasciation on chr 2 and chr 8 (*qKRN2* and *qKRN8*, respectively. Table 2) with kernel number increasing alleles dispersed between parental lines (from Lo964 and Lo1016, respectively). Many independent QTL mapping studies for the number of kernel rows has already been carried out and a thorough review is beyond the objectives of our study. However, it should be noted that a recent study cloned a major KRN QTL mapping on chr 2, just 10 Mb away from qKRN2 (Chen *et al.*, 2022). The gene was shown to encode for a member of the highly duplicated *WD40* gene and protein family, which play important role in diverse cellular functions like signal transduction, cell cycle control, intracellular transport, chromatin remodelling, cytoskeletal organization, and others. The authors verified that *WD40* alleles increasing the number of

kernel rows acted by increasing inflorescence meristem size, likely providing additional space for initiation of spikelet pair meristems and hence a higher number of kernel rows (Chen *et al.*, 2022). Given the close proximity (approx. 10 Mb) between *WD40* identified in Chen et al. (2022) and our QTL *qKRN2* in the subtelomeric region of chr 2, it will be certainly worth checking the effective identity/distinction between the two loci.

By cross-checking the QTL supporting intervals from our and other studies with the map positions of a number of inflorescence related candidate genes we identified a relatively short list of candidate genes possibly involved in explaining ear fasciation in the genetic background of our study, including *ramosa1* (*ra1*) (Dempewolf, 2010), *compact plant2* (*ct2*) (Bommert, Je, *et al.*, 2013), *big grain1 homolog1* (*bgh1*) (Simmons *et al.*, 2020), *barren inflorescence1* (*bif1*) (Barazesh and McSteen, 2008) etc (Fig. 4, Supp Table 2). The maize historical tassel and ear mutant *ra1*, encoding a zinc-finger transcriptional factor and producing ear and tassel with increased branches (Kim *et al.*, 2022) maps only 0.5 Mb away from the QTL cluster region including *qFas7*, and within the QTL supporting interval of *qKRN7.1*, thus *ra1* should be considered a very strong candidate gene to our *qFas7-qKRN7.1* QTL. This QTL region also appeared a hot region for ear fasciation and KRN, since many other authors mapped QTLs for these traits in this region (Fig. 4A). Due to artificial selection for thousands of years on ear shape (Sigmon and Vollbrecht, 2010), *ra1* is very poor of genetic diversity. However, ear formation is likely to be influenced by alteration in expression of *ra1*. For example, Liu et al (Liu *et al.*, 2019) found that *rel2* encoding a transcriptional co-repressor could dramatically increase the formation of long branches in ears of both *ra1* and *ra2* mutants. Comparison of genomic sequences between our three parental lines clearly showed lack of nucleotide sequence variation at *ra1* (Supp Figure 8). However, as shown in many studies, QTL are often due to allelic variation in gene expression level of the causative gene rather than from variation of coding allelic sequences (Salvi and Tuberosa, 2005; Jaganathan *et al.*, 2020), therefore, quantification of the expression of *ra1* in the ear primordium of Lo1016 and Lo964 will enable to test *ra1* involvement in ear fasciation driven by *qFas7*. Interestingly, *ra1* is not the only candidate gene mapping at *qFas7*, and other gene models, such as *Zm00001d020486* and *Zm00001d020461* due to their high expression level on ear inflorescence (Stelpflug *et al.*, 2016)

and inferred transferase activity of their orthologues in rice with relatively high FPKM in ear primordium will be considered for expression analysis such as thus requiring fine-mapping and analysis of expression levels.

Two potentially strong candidate genes, *compact plant2* (*ct2*) and *Big grain homolog1* (*bgh1*) were also identified within the supporting interval of *qFas1.2*. Maize lines carrying mutations at *ct2* produced fasciated ears (Bommert, Je, *et al.*, 2013), and the overexpression of *bgh1* resulted in increased ear kernel row number and total ear kernel number and mass, whereas individual kernels tended to developed slightly smaller (Zhang *et al.*, 2022), showing similar phenotypes of its rice ortholog *BG1* whose overexpression leads to significantly increased grain size (Liu, Tong, Xiao, *et al.*, 2015). Five common native *bgh1* alleles exhibit little structural and expression variation compared to the large increased expression conferred by these ectopic alleles (Simmons *et al.*, 2020). Distinct from the situation of *ra1*, preliminary analysis of sequencing data of three parent lines showed indel and substitution mutations in nucleotide and protein sequences of *ct2* and *bgh1* between Lo964 and Lo1016, however, no difference between B73 and Lo1016 coding sequences were observed, which is the genetic background where the QTL was detected (Table 2; Suppl Table 3). Thus also for this QTL, and for *ct2* and *bgh1*, we have to hypothesize either a difference in expression levels between the two alleles caused by variation at cis-regulatory elements or the presence in *qFas1.2* of other potential candidate genes affecting proliferation of ear primordium eventually causing ear fasciation.

In our study we dealt with ear prolificacy at single node, whereas other types of ear prolificacy include multi-stem/tillering, and multi-node prolificacy (Wang *et al.*, 2021). Single node ear prolificacy is clearly an architectural trait little investigated across maize genetics. At the same time, it is expected that the three types of ear prolificacy will likely require overlapping cell and tissue functions and therefore overlapping genes controlling them, suggesting the molecular genetics studies focusing on one single type of ear prolificacy will shed light on mechanisms acting also on the other types.

We noted in Introduction that ear prolificacy at the same node is due to the development of axillary buds at shank nodes/leaves (Ortez *et al.*, 2022). Variation in the number of ears at

the same node between maize genotypes could then be explained by a different level of apical dominance played by the main ear developing at the tip of the shank. Indeed, this is the typical explanation used to explain different numbers of ears at different node of the main plant stem between maize genotypes where the inhibitory effect on the activity of axillary buds below the tassel and the top ear is caused by basipetal transporting of indole-3-acetic acid in stems (Domagalska and Leyser, 2011). This would prevent underground axillary meristems to develop into tillers, and aboveground meristems to grow more ears in maize. However, whether this mechanism is acting on the ear shank to control ear prolificacy at single node has yet to be proved. In our study, four major QTL involved in prolificacy were mapped (Table 2; Fig. 3 and Supp Fig. 4 and 5). An overlap was observed between our *qProl4* and *prol4.1* by Wills (Wills *et al.*, 2013), despite no association with known genes inside this interval was established.

This notwithstanding, it is worth reporting that the gene *barren stalk fastigiate1* (*baf1*), a known gene that when mutated produces no ear shoots (Zhou *et al.*, 2021) maps very close to the north border of *qProl9* (Fig. 4B). Because of the known approximation behind QTL mapping, it is certainly worth carrying out further investigation on the possible connection between *baf1* and *qProl9*. Additionally, it is proved that *teosinte branched1* (*tb1*) does not only produce tassel-like ear branches, but also inhibits axillary bud growth as a repressor (Dong *et al.*, 2017).

More generally, it is well known how maize domestication proceeded from teosinte by suppressing the development of axillary branches by a profound increase in apical dominance. The teosinte plant has multiple long lateral branches, each tipped with a tassel. At each node along these lateral branches, there are clusters of several small ears. Summed over all branches, a single teosinte plant can easily have more than 100 small ears. By comparison, the maize plant has relatively few lateral branches (ie the two ear shanks), each tipped by a single large ear (in teosinte it would be a tassel) (Wills *et al.*, 2013). Using a set of 866 maize-teosinte BC2S3 recombinant inbred lines, Wills et al (2013) mapped eight ear prolificacy QTL, distributed across the first 5 chromosomes. One QTL on chromosome 1 (*prol1.1*) showed a much larger effect and accounted for 36.7% of the phenotypic variance. This QTL was shown to correspond to *grassy tillers1* (*gt1*) gene, which encodes a homeodomain leucine zipper

transcription factor. This information is crucial to begin understanding the regulatory mechanisms behind shoot branching in maize, and towards understanding the molecular genetic basis behind our *qProl* QTLs.

It is thought that tillering is highly related to the morphology and habit of growth of the perennial herbage grasses (Jewiss, 1972), with high scientific and application values. For example, tillering in rice (*Oryza sativa L.*) enables to improve grain production and is recognized as a model system for the study of branching in monocotyledonous plants (Li *et al.*, 2003). And Min et al (Xu *et al.*, 2005) identified a putative auxin efflux carrier, *OsPIN1* in rice, and either overexpression or inhibition of this gene in mutants influenced tiller numbers and shoot/root ratio. Studies of tillering in wheat (*Triticum aestivum* L.) have been also carried out for decades. However, compared with those two crops, a fewer number of studies addressed tillering in maize. In our study we mapped four TIL-associated QTL distributed on chromosome 1, 2, 4, and 9, mainly from the joint population. The negative additive effects of *qTil1*, *qTil4* and *qTil9* indicated major contribution of alleles of Lo1016, in line with the phenotype of three parent lines (Lo1016 is the only parent showing some tillering when grown in the field in standard conditions). However, the fact that the additive effects of *qTil2* is contributed by the B73 allele is apparently in contradiction with the observation that B73 develops virtually no tillers at least in our field conditions (Table 1). This observation suggests that at least some level of gene interaction occurs between tillering loci in our genetic materials, which should be subjected to future investigations.

Finally, it should be noted that while shoot branching producing ears and tillering clearly share developmental similarities (eg. both branching types originate from axillary buds of the stem nodes), in our study we did not find phenotypic correlation between ear prolificacy at single node and tillering (Fig. 2, Supp Fig. 1 and 2). Additionally, we did not find any overlaps between QTLs of the two traits. The most likely explanation is the specific genetic architecture of the genes involved in controlling the two traits in our genetic background. In other words, although it is likely that at least some genes in maize control the two traits with some pleiotropic effect, in our genetic background those genes did not segregate. Another factor, partially connected with this, is that the parental line contributing ear prolificacy (Lo964) showed

virtually no tillering, and the parental line contributing high tillering (Lo1016) showed no ear prolificacy, suggesting that each parental line possibly contributed in the segregating population strong (or relatively strong) alleles at gene acting only on one of the two traits.

5. CONCLUSION

In this study, a joint population consisting of 165 RIL lines developed starting from two experimental crosses with a parental line (source of ear fasciation) in common was utilized for the genetic dissection of ear fasciation, KRN, ear prolificacy and tillering. We identified solid positive correlation between ear fasciation and KRN, and provided evidence that the correlation was partially due to the pleiotropic effects of genes inducing inflorescence meristem fasciation at loci on chr 2 and chr 7. The fasciation effect of single ear fasciation QTL was mild and this likely contributed a positive effect on kernel row number, since it is well known that highly misshapen ears produced by plants carrying strong mutations at inflorescence meristem genes carry fewer kernel row numbers. We showed that our ear fasciation QTLs overlap with other fasciation and/or KRN QTL, which suggests that the genetic control of fasciation is not tremendously complex. Candidate genes were identified and alleles were compared between the three parental lines. However, we did not identify so far functional nucleotide polymorphism enabling to explain the strong phenotypic effects on fasciation and/or KRN observed, suggesting either that the selected candidate genes have nothing to do with fasciation or that functional variation lies in gene expression variation rather than nucleotide or amino acid variation.

Analysis for ear prolificacy at single node enabled us to identify four QTLs, of which one (on chr. 4) perfectly overlapped with an ear prolificacy identified in a former study in a maize × teosinte cross. The other three QTL mapped in novel chromosome regions previously unknown to control this trait. Quite unexpectedly, we did not find correlation and QTL map overlaps between ear prolificacy and tillering, although the two traits share obvious developmental basis. The genetic architecture of the trait in this specific genetic background likely cause the lack of correlation and QTL overlaps. Overall, our study provided clear entry

points for the molecular dissection of important yield component traits, which should help both developing molecular markers for marker-assisted selection to be deployed in breeding programs and starting the procedures leading to cloning the genes underpinning the here described QTLs.

Some notable co-localizations between our QTLs and known functional genes, such as qFas7 – qKRN7.1 and ramosa1, were observed in our result datasets, in spite of the modest effects of QTLs compared with the potentially stronger effects of genes around. Thus, our results are in line with the so-called Robertson's hypothesis (Robertson 1985) which hypothesized that a QTL can be generated by a minor mutant allele at a Mendelian locus known thanks to the presence and the former characterization of major mutant allele(s). This hypothesis was extended by Schnable et al. (Schnable and Freeling 2011), who suggested that strong-effect QTLs should most frequently correspond to syntenic genes, whereas weaker-effect QTLs should correspond to non-syntenic ones, such as the genes identified in Tai et al. (Tai et al. 2016). In hence, the latter ones are usually regarded as regulation factors (or modifiers) of functional genes, such as ramosa1 enhancer locus2 (rel2) positioned on chromosome 10 (Gallavotti et al. 2010). For instance, rel2 mutants can dramatically increase the formation of long branches in ears of both ra1 and ra2 mutants (Liu et al. 2019), suggesting the upregulation role in the ramosa pathway.

Acknowledgement

Time flies away so fast before realizing. It seems that I might stay in Italy, enjoy coffee and pizza, watch Seire A as if I were doing in the past four years. Honestly, these four years do affect my lifestyle and life attitude deeply. For example, I started taking short trips with friends during weekends gradually rather than just staying at home. Or, I have tried to made some Italian food by myself rather than only tasting Chinese food. What I learned during these years is that it is not worth filling your life only with work. It is better to improve your quality of life by enjoying something interesting, like delicious food, beautiful travelling and so on.

Of course, I must express my gratitude to my colleagues. They really did a lot of things to help me, not only on studies, but also on living.

Thanks to Alberto. I would remember the time when we worked in the maize filed to do the selfing and shovelomics forever. And after coming back to the greenhouse, you also helped me to deal with some tiny but annoying stuff.

Thanks to Serena. You are so kind for everything, I have to say. I am really sorry to disturb you to help me call Italian number for everything. Besides, your work contributing to SNP calling improved this thesis a lot.

Thanks to Christian. Your rich experience on gene expression and sequencing did help me overcome a lot of difficulties, and improve the efficiency a lot.

Who I want to thank a lot are Prof. Silvio. He is a real gentleman and glad to help others. When I got in difficulties, related to unibo stuff for example, he always sent an email or call the number to make it clear. Additionally, he is a good friend in life. We are always chatting on something interesting.

Also, thanks to my familes although I could not see them due to the pandemic, which makes me miss them a lot. And I really accompany with them for some time.

In the end, I would say, I do appreciate the experience in this lab. I do appreciate the viewing in this country. Wish I could visit Italy again in future!

Tables and Figures

Table 1 Descriptive statistics for plant architecture and ear traits in the two RIL populations B73 × Lo1016 (B×L) and Lo964 × Lo1016 (L×L).

	B73	Lo964	Lo1016	B73 × Lo1016		Lo964 × Lo1016	
	Mean ± sd	Mean ±sd	Mean ± sd	Min - Mean - Max	h^2	Min - Mean - Max	h^2
DIA	0.95 ± 0.04 (a)	0.95 ± 0.04 (a)	0.85 ± 0.11 (a)	0.86 - 0.94 - 0.98	0.45	0.88 - 0.95 - 0.98	0.13
DIS	7.17 ± 1.18 (a)	6.33 ± 1.89 (a)	7.18 ± 0.94 (a)	2.75 - 6.02 - 8.89	0.58	3 - 5.25 - 8.61	0.63
FAS	0.18 ± 0.39 (a)	0.50 ± 0.50 (a)	2.20 ± 0.75 (b)	0 - 1.38 - 3	0.95	0 - 0.79 - 2.92	0.94
KRN	16.33 ± 1.20 (a)	14.54 ± 1.03 (a)	19.75 ± 1.71 (b)	14.58 - 17.40 - 20.90	0.59	12.67 - 15.97 - 20.13	0.85
OVA	5.85 ± 1.03 (a)	4.92 ± 1.82 (a)	7.13 ± 1.17 (b)	4.1 - 6.02 - 8.11	0.5	3.69 - 5.60 - 8.11	0.55
PROL	0 ± 0 (a)	2.75 ± 2.36 (b)	0.25 ± 0.5 (a)	0 - 0.40 - 1	0.41	0 - 0.59 - 1	0.78
TIL	0 ± 0 (a)	0 ± 0 (a)	1.5 ± 2.38 (b)	0 - 1.22 - 5.75	0.62	0 - 1.24 - 5.25	0.68

DIA (ear diameters rate), DIS (kernel row disorder), OVA (ear ovality), FAS (ear fasciation index), KRN (kernel row number), PROL (prolificacy), TIL (number of tillers).

Table 2 QTL results for ear-fasciation (and related traits), kernel row number, ear prolificacy and tillering as obtained by composite interval mapping using BLUES-modifed phenotypic values, on single RIL populations (B×L and L×L) and by analysis of joint population (JP).

Trait type	QTL	Trait	Source[a]	Genetic[b]	Bin	Physical B73v4Gramene	LOD[c]	PVE[d]	LOD B×L[e]	LOD L×L[f]	Add B×L[g]	Add L×L[h]
Ear fasciation and KRN	*qFas1.1*	Ear diameter rate	B×L	chr1:18	1.01	1:4,727,090..5,522,697	3.97	13.35			0.01	
	qFas1.2	Fasciation	B×L	chr1:40	1.02	1:16,049,788..18,019,336	4.23	17.53			-0.33	
	qKRN2	Kernel row number	JP	chr2:18.8	2.02	2:4,139,916..4,808,238	5.77	13.23		5.45		0.69
		Kernel row number	L×L	chr2:27	2.02	2:4,335,580..5,766,846	7.76	22.99				0.87
	qFas5	Fasciation	L×L	chr5:114	5.07	5:210,666,787..211,006,289	4.09	21.70				-0.24
		Ovality	JP	chr5	5.07	5:216,124,262..218,020,826	4.51	11.41	1.88	2.64	-0.21	-0.34
	qKRN5	Kernel row number	L×L	chr5:154	5.07	5:217,164,610..218,092,335	3.83	10.01				-0.57
	qKRN7.1	Kernel row number	L×L	chr7:131	7.02	7:110,164,470..123,888,193	4.33	11.80				-0.62
	qFas7	Fasciation	JP	chr7:32.8	7.02	7:114,986,412..118,589,566	6.95	10.92	3.20	3.75	-0.23	-0.24
		Fasciation	B×L	chr7:44	7.02	7:114,986,412..118,512,477	4.58	19.41			-0.35	
		Disorder	JP	chr7:34.2	7.02	7:115,485,353..123,389,126	5.18	10.51	3.11	2.08	-0.43	-0.41
		Ovality	JP	chr7:39.4	7.02	7:125,598,407..125,842,182	4.65	11.48	*1.79*	2.85	*-0.19*	-0.36
	qKRN7.2	Kernel row number	JP	chr7:93.7	7.03	7:149,411,478..150,243,845	5.27	8.77		4.94		-0.65
	qKRN8	Kernel row number	L×L	chr8:34	8.02	8:18,827,357..20,248,512	6.29	17.88				-0.79

		Kernel row number	JP	chr8:23.5	8.02	8:19,522,583..20,248,512	4.71	8.30		4.53		-0.63
Tillering	*qTil1*	Tillering	JP	chr1:110.0	1.05	1:85,069,032..94,479,235	7.59	12.15	3.06	4.53	-0.40	-0.57
		Tillering	L×L	chr1:118.0	1.05	1:96,638,867..164,032,566	4.45	22.25				-0.85
	qTil2	Tillering	JP	chr2:7.3	2.01	2:2,067,198..3,242,152	7.05	13.08	6.42		0.58	
		Tillering	B×L	chr2:9	2.01	2:2,802,567..4,139,916	6.93	18.38			0.70	
	qTil4	Tillering	JP	chr4:115.9	4.04/05	4:30,890,749..37,691,500	6.70	10.66	3.19	3.51	-0.41	-0.51
	qTil9	Tillering	JP	chr9:67.5	9.03	9:92,749,841..97,243,143	6.19	9.50	3.40	2.79	-0.42	-0.45
Prolificacy	*qProl1*	Prolificacy	L×L	chr1:2.0	1.01	1:6,272,408..7,074,707	6.07	5.58				-0.34
	qProl2	Prolificacy	JP	chr2:139.2	2.06/7	2:187,831,696..191,179,806	6.34	13.97	4.52	*1.82*	0.13	*0.11*
	qProl4	Prolificacy	L×L	chr4:371.1	4.05/4.08	4:148,677,638..181,859,161	6.22	5.74				-0.34
	qProl9	Prolificacy	B×L	chr9:62	9.03	9:28,670,077..74,515,763	3.64	16.72			-0.21	

[a]) Actual population (B×L, L×L or JP, with JP indicating the two populations jointly analyzed for QTL using the command 'NAM' in QTL Icimapping.

[b]) QTL peak position in cM in the specific linkage map (B×L, L×L or JP, from this study)

[c]) Peak LOD value from Composite Interval Mapping.

[d]) PVE = Proportion of phenotypic variance explained.

[e]) Peak LOD value of the single population B×L when analysed as JP. Sub-significant relevant LOD score are in Italics.

[f]) Peak LOD value of the single population L×L when analysed as JP. Sub-significant relevant LOD score are in Italics.

[g]) QTL additive effect express as 2a = (mean homozygous B73 – mean homozygous Lo1016). Additive values related with sub-significant LOD scores are in Italics.

[h]) QTL additive effect express as 2a = (mean homozygous Lo964 – mean homozygous Lo1016). Additive values related with sub-significant LOD scores are in Italics.

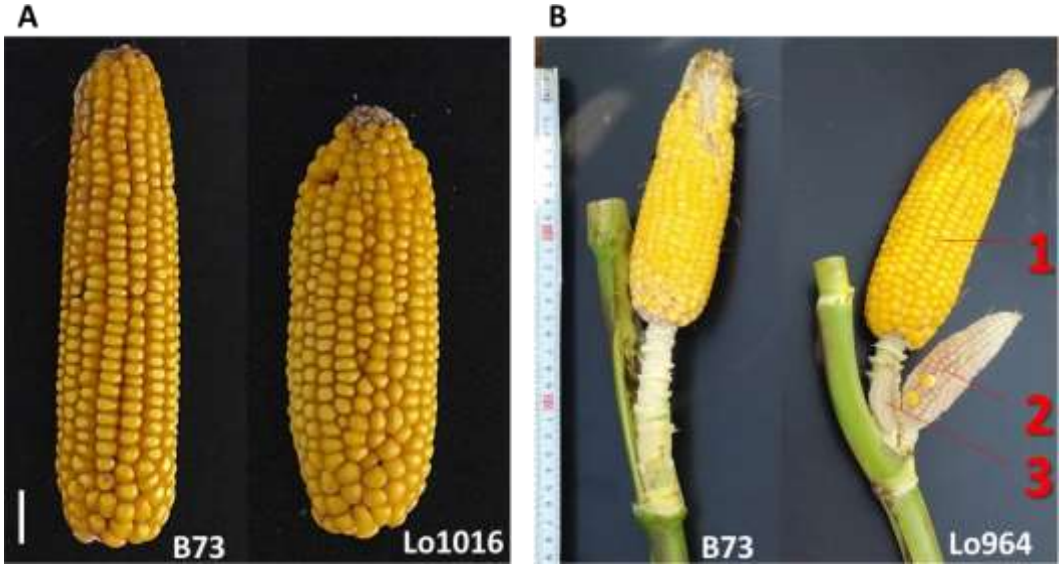

Figure 1. Target ear traits analyzed in this study. (A) Representative images of the ear-fasciation phenotype observed in Lo1016 (B73 is shown as comparison). White line, 10cm. (B) Representative images of the ear prolificacy phenotype at top ear-bearing node as observed in Lo964 (B73 is shown as comparison).

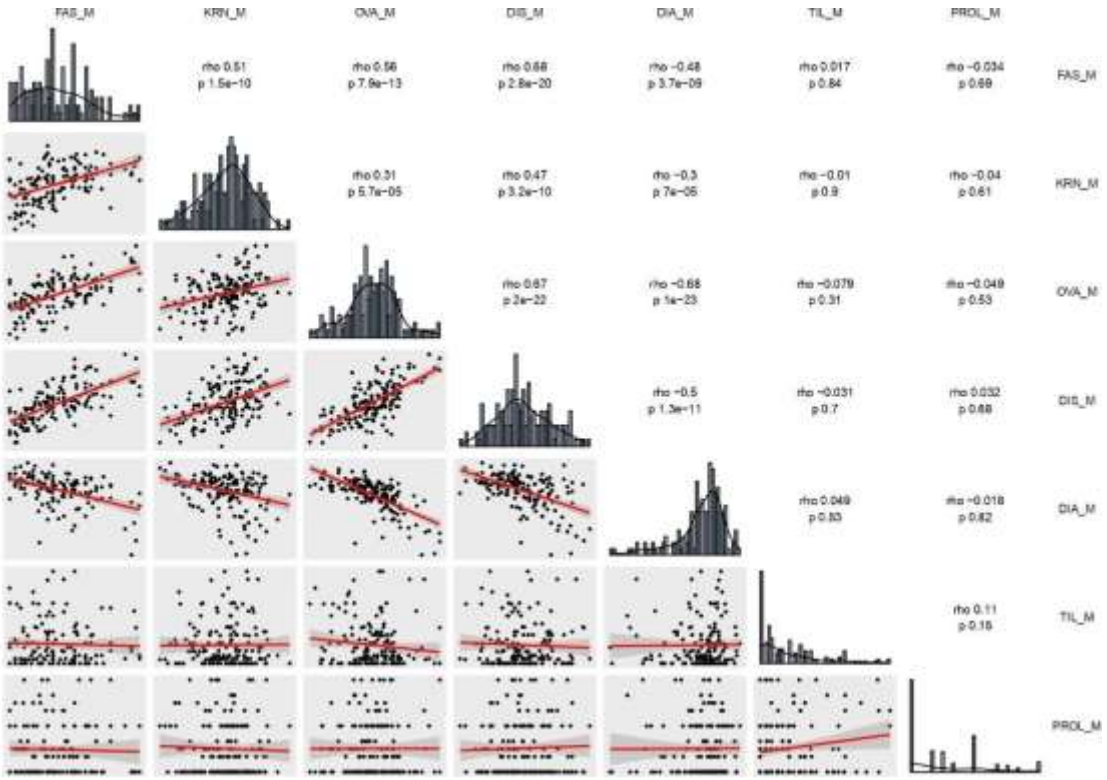

Figure 2. Distribution frequency histograms of, and correlation (Spearman) among all traits estimated on the two RILs (B×L and L×L) combined.

The upper right part presents all correlation indexes (*rho*, thus the upper number) and corresponding significant levels (*p*, thus the lower number). Minus rho values show negative correlation between two traits, and vice versa. The lower left part presents scatter plots and fitter curve (the red line inside) between two traits. The diagonal shows histogram charts of each trait. DIA (ear diameters rate), DIS (kernel row disorder), OVA (ear ovality), FAS (ear fasciation index), KRN (kernel row number), PROL (prolificacy), TIL (number of tillers), M, mean value.

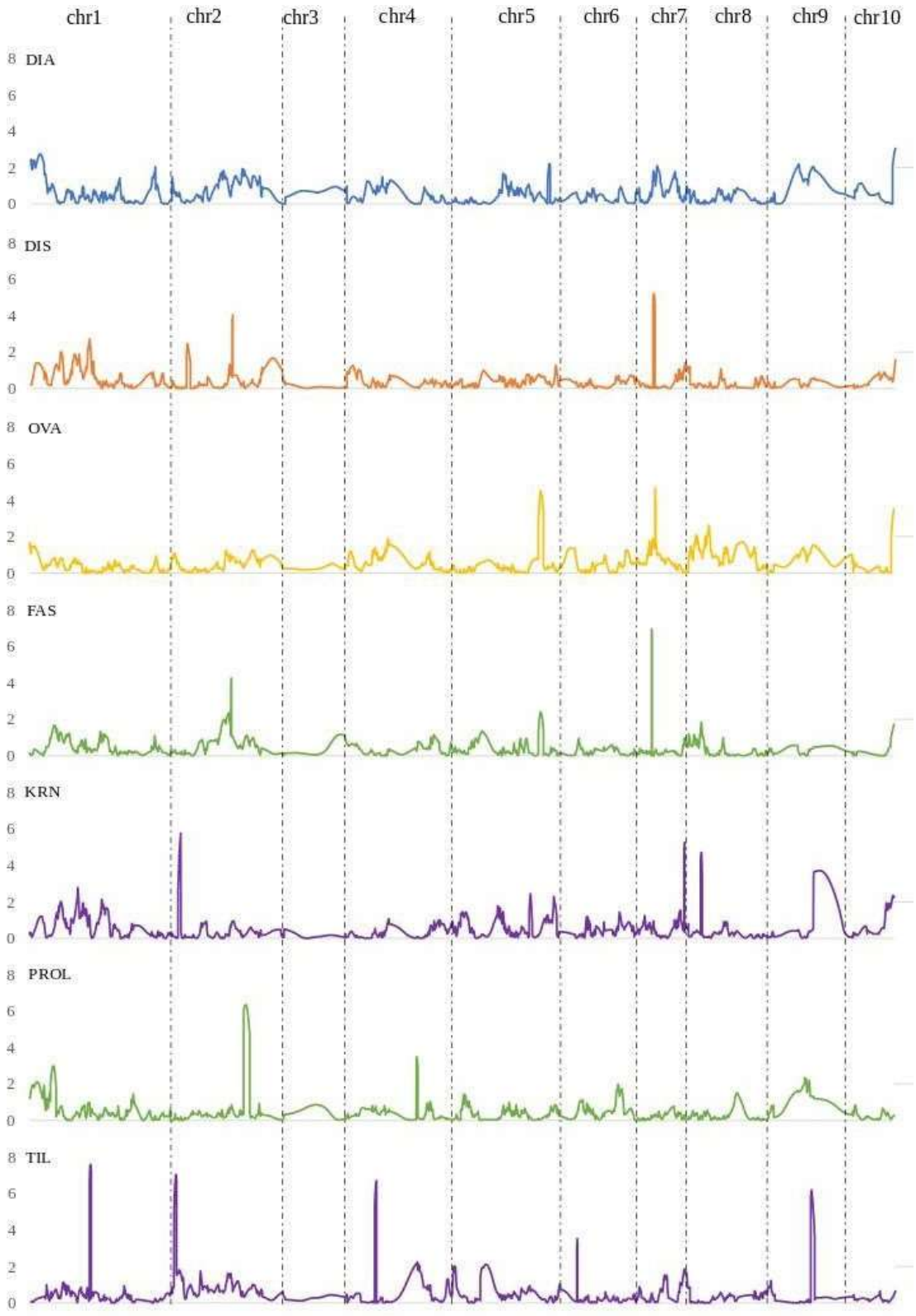

Figure 3. QTL LOD profiles obtained by the joint analysis of the two RIL populations B×L and L×L, for DIA (ear diameters rate), DIS (kernel row disorder), OVA (ear ovality), FAS (ear fasciation index), KRN (kernel row number), PROL (prolificacy), TIL (number of tillers).

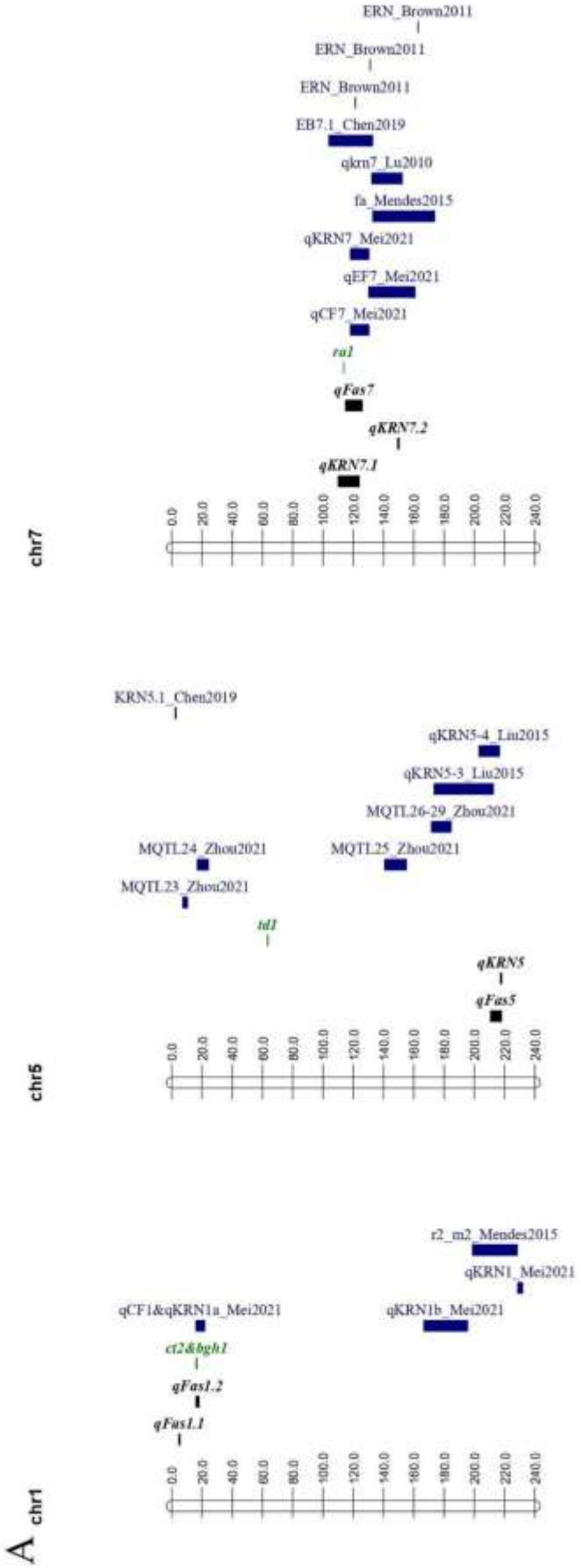
ERN_Brown2011
ERN_Brown2011
ERN_Brown2011
EB7.1_Chen2019
qkrn7_Lu2010
fa_Mendes2015
qKRN7_Mei2021
qEF7_Mei2021
qCF7_Mei2021
ra1
qFas7
qKRN7.2
qKRN7.1
0.0 20.0 40.0 60.0 80.0 100.0 120.0 140.0 160.0 180.0 200.0 220.0 240.0
chr7
KRN5.1_Chen2019
qKRN5-4_Liu2015
qKRN5-3_Liu2015
MQTL26-29_Zhou2021
MQTL24_Zhou2021
MQTL25_Zhou2021
MQTL23_Zhou2021
td1
qKRN5
qFas5
0.0 20.0 40.0 60.0 80.0 100.0 120.0 140.0 160.0 180.0 200.0 220.0 240.0
chr5
r2_m2_Mendes2015
qKRN1_Mei2021
qCF1&qKRN1a_Mei2021
qKRN1b_Mei2021
ct2&bgh1
qFas1.2
qFas1.1
0.0 20.0 40.0 60.0 80.0 100.0 120.0 140.0 160.0 180.0 200.0 220.0 240.0
chr1

A

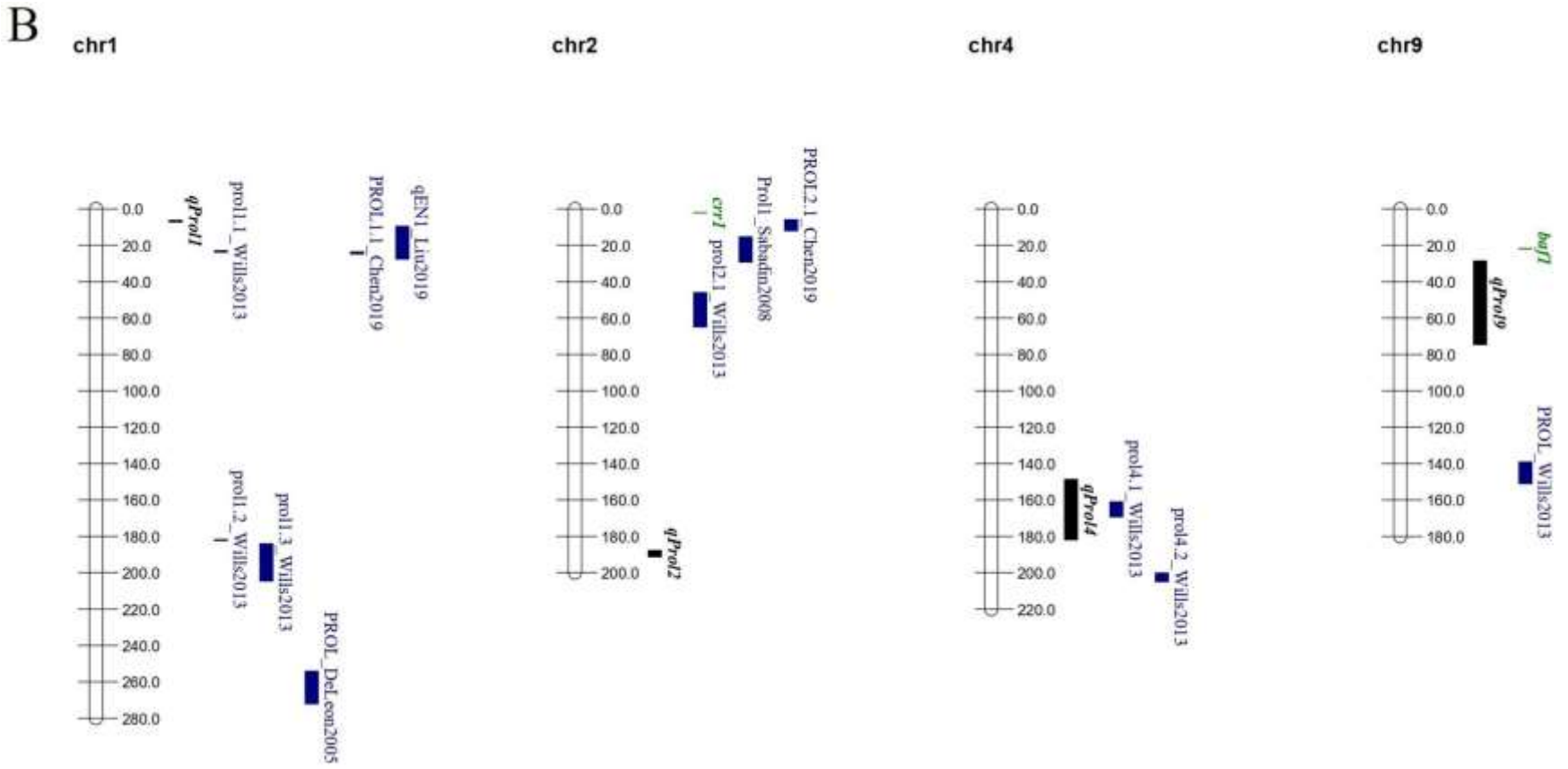

Figure 4. QTL consensus maps. (A) QTL consensus map for ear fasciation including QTL from literature and this study. (B) QTL consensus map for ear prolificacy, including QTL from literature and from this study. Chromosome bars and numbers represent physical distances in Mb. QTL positions are

represented following physical positions reported in Table 3. In black, QTL from this study; in green, tentative candidate genes; in blue, QTL from other studies.

Supplementary Tables and Figures

Supplementary Table1 Information of genetic maps of three populations

Chr	B×L			L×L			JP		
	Marker	Length	mean cM	Marker	Length	mean cM	Marker	Length	mean cM
1	195	329.18	1.69	164	286.48	1.75	199	260.90	1.31
2	186	224.46	1.21	141	281.82	2.00	100	209.82	2.10
3	81	166.34	2.05	13	133.72	10.29	6	114.03	19.01
4	155	229.12	1.48	93	292.55	4.76	99	217.82	2.20
5	128	176.48	1.38	107	187.03	1.75	120	177.90	1.48
6	107	150.96	1.41	86	181.76	2.11	80	142.91	1.79
7	84	109.41	1.30	116	324.77	2.80	104	100.91	0.97
8	100	168.64	1.69	93	232.69	2.50	112	157.31	1.40
9	75	143.68	1.92	32	248.49	7.77	24	147.28	6.14
10	80	121.25	1.52	34	132.43	3.90	26	75.68	2.91
total	**1191**	**1819.52**	**1.53**	**890**	**2504.45**	**2.81**	**885**	**1661.00**	**1.88**

Supp Table 2. Information on most important known genes involved in ear fasciation, ear prolificacy and tillering

Candidate genes	Gene model in B73 v3	Gene model in B73 v4 Gramene	Genomic position in B73 v4	bin	Ref.
FASCIATION AND NUMBER OF KERNEL ROWS					
fea3	GRAZM2G166524	Zm00001d040130	Chr3: 28,711,131..28,713,322)	3.04	Jackson, D and Hake, S (1999) The genetics of ear fasciation in maize. 73:2
fea2	GRMZM2G104925	Zm00001d051012	Chr4: 136,765,871..136,767,872)	4.05	Jackson, D and Hake, S (1999) The genetics of ear fasciation in maize. 73:2
cle7 - clavata3/esr-related7	GRMZM2G372364		Chr4: 7,570,324..7,571,104)	4.02	Tran et al. 2020 Genes , 11(3), 281; https://doi.org/10.3390/genes11030281
fcp1 (fon2-like cle protein1)	GRMZM2G165836	Zm00001d003320	Chr2: 40,126,366..40,127,328	2.04	Je, Byoung Il et al. 2020. Maize Genetics Conference Abstracts 62:P166
fea4 - fasciated ear4	GRMZM2G133331	Zm00001d037317	Chr6: 120,714,112..120,726,773	6.04	Allen, SM et al. 2013. Patent WO2013138544A1
td1 - thick tassel dwarf1	GRMZM2G300133	Zm00001d014793	Chr5: 63,456,839..63,460,120	5.03	Lunde, C; Hake, S. 2006. Maize Genetics Conference Abstracts. 48:P122
ct2 - compact plant2	GRMZM2G064732	Zm00001d027886	Chr1: 16,722,714..16,730,676	1.02	Bommert, P; Yin, P; Jackson, D. 2010. Maize Genetics Conference Abstracts. 52:P119
ub2 - unbranched2	GRMZM2G160917	Zm00001d031451	Chr1: 190,382,866..190,386,589	1.06	Chuck GS, Brown PJ, Meeley R, Hake S. Maize SBP-box transcription factors unbranched2 and unbranched3 affect

					yield traits by regulating the rate of lateral primordia initiation. Proceedings of the National Academy of Sciences. 2014 Dec 30;111(52):18775-80.
ub3 - unbranched3	GRMZM2G460544	Zm00001d052890	Chr4: 203,611,347..203,615,518	4.08	Chuck GS, Brown PJ, Meeley R, Hake S. Maize SBP-box transcription factors unbranched2 and unbranched3 affect yield traits by regulating the rate of lateral primordia initiation. Proceedings of the National Academy of Sciences. 2014 Dec 30;111(52):18775-80.
gif1 - growth-regulating-factor-interacting factor1	GRMZM2G180246	Zm00001d033905	Chr1: 278,134,999..278,138,569	1.01	Zhang, D, et al. 2018. Plant Cell. 0:doi: 10.1105/tpc.17.00791
dcl101 - dicer-like 101	GRMZM2G040762	Zm00001d027412	Chr1: 4,724,456..4,736,832	1	Thompson, BE et al. 2014. Plant Cell 26:4702-4717
cg1 - corngrass1	GRMZM2G022489		Chr3: 6,928,278..6,928,401	3.02	Abedon, B and Tracy, WF. 1995. MNL 69:97-98
crn1 - coryne1	GRMZM2G032132	Zm00001d042268	Chr3: 158,268,237..158,272,672	3.05	Je BI, Xu F, Wu QY, Liu L, Meeley R, Gallagher JP, Corcilius L, Payne RJ, Bartlett ME, Jackson D (2018) The CLAVATA receptor FASCIATED EAR2 responds to distinct CLE peptides by signaling through two downstream effectors. Elife 7: e35673
ra1 - ramosa1	GRMZM2G003927	Zm00001d020430	Chr7: 113,572,410..113,572,937	7.02	Vollbrecht, E and Martienssen, RA. 2000. Maize Genetics Conference Abstracts 42:P74

rel1 - ramosa1 enhancer locus1				1.07	https://www.maizegdb.org/data_center/locus/9020728	
rel2 - ramosa1 enhancer locus2	GRMZM2G042992	Zm00001d024523	Chr10: 75,993,828..76,002,912	10.03	Gallavotti, A; et al. 2008. Maize Genetics Conference Abstracts. 50:T15	
ZmGB1 - heterotrimeric G protein beta, gbp2 (GTP binding protein2)	GRMZM2G045314	Zm00001d033422	Chr1: 262,592,398..262,598,732	1.09	Wu et al 2020 The maize heterotrimeric G protein subunit controls shoot meristem development and immune responses. Proc. Natl. Acad. Sci. USA 2020, 117, 1799–1805	
C2H2-type zinc finger transcription factor related to RAMOSA1 (RA1)	GRMZM2G361210	Zm00001d034642	Chr1: 298,700,432..298,700,869	1.11	Xu et al 2021	YES, metaclusters 9-10-11
ZmTMO5 Arabidopsis homolog controls periclinal cell divisions during vascular development	GRMZM2G043854	Zm00001d047878	Chr9: 144,091,969..144,094,962	9.06	Xu et al 2021	YES, metaclusters 9-10-12
yab9 - yabby9	GRMZM2G074543	Zm00001d013895	Chr5:24,089,489..24,093,556	5.03	Xu et al 2021	YES, metaclusters 9-10-12

Ra3 Ramosa3, trehalose-6-phosphate phosphatas	GRMZM2G014729	Zm00001d022193	Chr7: 172,484,959..172,489,194)	7.04	Satoh, N and Jackson, D. 2003. Developmental analysis of the ramosa3-fasciated ear 1 mutant. Maize Genetics Conference Abstracts 45:P104
Ra2 Ramosa2,	AC233943.1_FG002	Zm00001d039694	Chr3:12,158,280..12,159,065	3.02	Bortiri, E, et al. 2006. Plant Cell. 18:574-585
tassels replace upper ears1 (tru1) - Arabidopsis BLADE-ON-PETIOLE (BOP1) Ankyrin repeat	GRMZM2G039867	Zm00001d042111	Chr3: 151,328,862..151,332,856	3.05	Dong, Z. B. et al. Ideal crop plant architecture is mediated by tassels replace upper ears1, a BTB/POZ ankyrin repeat gene directly targeted by TEOSINTE BRANCHED1. Proc. Natl Acad. Sci. USA 114, E8656–E8664 (2017).
ts2 - tassel seed2	GRMZM2G455809	Zm00001d028806	Chr1:46,955,327..46,956,671	1.03	Irish, EE and Nelson, TM. 1993. Am J Bot 80:292-299
bif2 - barren inflorescence2	GRMZM2G171822	Zm00001d031068	Chr1:175,807,851..175,809,432	1.05	McSteen, P et al. 2007. Plant Physiol 144: 1000-1011
an1 - anther ear1	GRMZM2G081554	Zm00001d032961	Chr1:244,858,795..244,867,417	1.08	Zhou, LZ et al. 2017. Molecular Plant pp.doi: 10.1016/j.molp.2017.01.012
ts1 - tassel seed1	GRMZM2G104843	Zm00001d003533	Chr2:47,105,187..47,109,372	2.04	Hultquist, J; Dorweiler, JE. 2008. Planta. 229:99-113
D8 - dwarf plant8	GRMZM2G144744	Zm00001d033680	Chr1:270,918085..270,919,977	1.10	Sakai, S; Katsumi, M. 1994. Biosci Biotechnol Biochem 58:1340-1342
kn1 - knotted1	GRMZM2G017087	Zm00001d033859	Chr1:276,073,335..276,081,242	1.10	Hake, S and Freeling, M. 1986. Nature 320:621-623

ts6 - tasselseed6	GRMZM5G862109	Zm00001d034629	Chr1:298,422,859..298,427,050	1.11	tephenson, E et al. 2019. PLoS One 14:e0203728
zfl1 - zea floricaula/leafy	GRMZM2G098813	Zm00001d026231	Chr10:141,561,862..141,564,767	10.06	Stephenson, E et al. 2019. PLoS One 14:e0203728
zfl2 - Zea floricaula leafy2	GRMZM2G180190	Zm00001d002449	Chr2:12,914,091..12,917,068	2.02	Yang, HL et al. 2021. Plant Physiol pp.doi: 10.1093/plphys/kiab557
ts4 - tasselseed4	GRMZM5G803935		Chr3:144,918,011..144,918,720	3.04	Xu, DY et al. 2017. Molecular Plant pp.doi: 10.1016/j.molp.2017.09.016
te1 - terminal ear1	GRMZM2G085113	Zm00001d042445	Chr3:167,821,561..167,825,000	3.05	Laureyns, R et al. 2021. Plant Physiol pp.doi:10.1093/plphys/kiab533
lg2 - liguleless2	GRMZM2G060216	Zm00001d042777	Chr3:179,387,727..179,396,447	3.06	Strable, J; Nelissen, H. 2021. Curr Opin Plant Biol 63:102038
ba1 - barren stalk1	GRMZM2G397518	Zm00001d042989	Chr3:186,014,629..186,015,264	3.06	Stroud, LK; McGinnis, K. 2017. Plant Direct. DOI: 10.1002/pld3.19
spi1 - sparse inflorescence1	GRMZM2G025222	Zm00001d044069	Chr3:218,287,295..218,289,461	3.08	Laureyns, R et al. 2021. Plant Physiol pp.doi:10.1093/plphys/kiab533
tga1 - teosinte glume architecture1	GRMZM2G101511	Zm00001d049822	Chr4:46,350,597..46,355,118	4.05	Kim, DE et al. 2022. J Plant Biol pp.doi: 10.1007/s12374-021-09342-1
tsh1- tassel sheath1	GRMZM2G325850	Zm00001d039113	Chr6:170,248,013..170,249,485	6.07	Zhou, Y et al. 2021. Plant Cell pp.doi: 10.1093/plcell/koab134

tsh4 - tassel sheath4	GRMZM2G307588	Zm00001d020941	Chr7:137,273,600..137,277,139	7.03	Stephenson, E et al. 2019. PLoS One 14:e0203728
dlf1 - delayed flowering1	GRMZM2G067921	Zm00001d022613	Chr7:181,089,568..181,090,715	7.06	Zhou, Y et al. 2021. Plant Cell pp.doi: 10.1093/plcell/koab134
bd1 - branched silkless1	GRMZM2G307119	Zm00001d022488	Chr7:178,605,958..178,606,905	7.04	Zhou, Y et al. 2021. Plant Cell pp.doi: 10.1093/plcell/koab134
EAR PROLIFICACY					
baf1 - barren stalk fastigiate1	GRMZM2G072274	Zm00001d045427	Chr9:21,784,850..21,788,875	9.02	Gallavotti, A et al. 2011. Plant Cell 23:1756-1771
TILLERING					
gt1 - grassy tillers1	GRMZM2G005624	Zm00001d028129	Chr1: 23,625,801..23,627,370	1.02	Laureyns, R et al. 2021. Plant Physiol pp.doi:10.1093/plphys/kiab533
teosinte branched1 (tb1)	AC233950.1_FG002	Zm00001d033673	Chr1:270,553,676..270,554,776	1.09	Doebley, J; Stec, A; Gustus, C. 1995. Genetics 141:333-346
tassels replace upper ears1 (tru1) - Arabidopsis BLADE-ON-PETIOLE (BOP1)	GRMZM2G039867	Zm00001d042111	Chr3:151,328,862..151,332,856	3.05	Dong, Z. B. et al. Ideal crop plant architecture is mediated by tassels replace upper ears1, a BTB/POZ ankyrin repeat gene directly targeted by TEOSINTE BRANCHED1. Proc. Natl Acad. Sci. USA 114, E8656–E8664 (2017).

tin1 - C2H2-zinc-finger transcription factor	GRMZM2G059088	Zm00001d018816	Chr7:6,104,753..6,105,325	7.01	Zhang X, Lin Z, Wang J, Liu H, Zhou L, Zhong S, Li Y, Zhu C, Liu J, Lin Z. The tin1 gene retains the function of promoting tillering in maize. Nature communications. 2019 Dec 6;10(1):1-3.
RELK1 (tpl1 - topless-related1)	GRMZM2G316967	Zm00001d040279	Chr3: 35,510,649..35,520,277	3.04	Zhang X, Lin Z, Wang J, Liu H, Zhou L, Zhong S, Li Y, Zhu C, Liu J, Lin Z. The tin1 gene retains the function of promoting tillering in maize. Nature communications. 2019 Dec 6;10(1):1-3.
RELK2	GRMZM2G030422	Zm00001d028481	Chr1:36,474,424..36,485,449	1.03	Zhang X, Lin Z, Wang J, Liu H, Zhou L, Zhong S, Li Y, Zhu C, Liu J, Lin Z. The tin1 gene retains the function of promoting tillering in maize. Nature communications. 2019 Dec 6;10(1):1-3.
REL2-RAMOSA1 ENHANCER LOCUS2	GRMZM2G042992	Zm00001d024523	Chr10: 75,993,828..76,002,912	10.03	Zhang X, Lin Z, Wang J, Liu H, Zhou L, Zhong S, Li Y, Zhu C, Liu J, Lin Z. The tin1 gene retains the function of promoting tillering in maize. Nature communications. 2019 Dec 6;10(1):1-3.

Supplementary Table 3.

QTL	Traits and QTL effect direction	Supporting interval	Gene	Gene model v4	Gene model v5	Position	Description	SNP and aminoacid differences between B73 and Lo1016	SNP and aminoacid differences between Lo964 and Lo1016
qFas1.1	Diameter rate, B×L, '+' fasciation by Lo1016	1:4,727,090..5,522,697	zag6 (agamous-like6)	Zm00001d027425	Zm00001eb001670	1:4,979,131..4,994,850	Encodes a MADS-box transcription factor homologous to SUPPRESSOR OF OVEREXPRESSION OF CONSTANS 1 that affects flowering time in Arabidopsis	In progress	In progress
			dcl101 (dicer-like 101)	Zm00001d027412	Zm00001eb001570	1:4,724,456..4,736,832	mutant plants have 'fuzzy tassel' and reduced stature.	In progress	In progress
			uce3 (ubiquitin conjugating enzyme3)	Zm00001d027427	Zm00001eb001680	1:5,095,291..5,099,640	is downstream of zagl1 (zag6); encodes an ubiquitin-conjugating enzyme with homology to Arabidopsis thaliana	In progress	In progress

							SUMO-conjugating enzyme 1 (AtSCE1; Wills et al, 2017)		
qFas1.2	Ear Fasciation. B×L, '+' fasciation by Lo1016	1:16,049,788..18,019,336	ct2 - compact plant2	Zm00001d027886	Zm00001eb005840	1:16,722,714..16,730,676	semi-dwarf plant, 1/3 height; shortened internodes; club tassel, fasciated ear	No difference	3SNP & 3 AA substitution
			bgh1 (big grain1 homolog1)	Zm00001d027877	Zm00001eb005840	1:16,284,218..16,285,168	overexpression is associated with increased ear kernel row number and total ear kernel number and mass	No difference	33SNP & 11 AA substitution
qKRN7.1/qFas7	Fasciation, disorder, ovality, KRN. L×L and B×L, '+' fasciation and KRN by Lo1016	7:110,164,470..123,888,193	ra1(ramosa1)	Zm00001d020430	Zm00001eb312340	7:113,572,410..113,572,937	ear and tassel many-branched; tassel branches taper to tip	No difference	No difference

qKRN8	KRN. L×L,JP, '+' KRN by Lo1016	8:18,827,357..20,248,512	bif1 (barren inflorescence1)	Zm00001d008749	Zm00001eb336930	8:18,951,758..18,953,833	dominant Bif1 plants have ear and tassel with many fewer spikelets, bare rachis appendages	No difference	No difference
qTil2	Tiller. B×L, JP, '+' Tiller by B73	2:2,067,198..4,139,916	crr1 (cytokinin response regulator1)	Zm00001d001865	Zm00001eb066570	2:2,078,887..2,079,669	involved in nitrogen signal transduction	No difference	6SNP & 6 AA substitution
			arftf3 (ARF-transcription factor 3)	Zm00001d001879	Zm00001eb066640	2:2,248,003..2,257,574	Auxin response factor	In progress	In progress

Supp Table 4. Information on QTL for KRN and ear fasciation from literature

Trait	QTL name	Original cross	population type	Chr.	BIN	Genetic Pos	Left marker	Right marker	Left position	Right position	Peak position	Reference
KRN	MQTL_KRN_6			2	2.03	220.48	ole1	IDP296	22,072,283	29,993,501		Zhou et al. 2021
KRN	MQTL_KRN_7			2	2.05	345.11	umc1581	IDP8112	73,594,726	102,943,993		Zhou et al. 2021
KRN	MQTL_KRN_8			2	2.06	376.21	IDP735	umc1755	156,821,566	179,457,271		Zhou et al. 2021
KRN	MQTL_KRN_23			5	5.01	141.48	phyC2	umc1587	7,382,139	10,404,954		Zhou et al. 2021
KRN	MQTL_KRN_24			5	5.03	219.01	mbd109	mmp180	16,891,070	24,173,911		Zhou et al. 2021
KRN	MQTL_KRN_25			5	5.04	322.07	TIDP8860	pza00270	140,717,468	155,133,354		Zhou et al. 2021
KRN	MQTL_KRN_26			5	5.04	362.19	ppi1	IDP1648	171,711,252	173,177,267		Zhou et al. 2021
KRN	MQTL_KRN_27			5	5.04	387.08	aasr6	TIDP5775	175,170,821	176,050,924		Zhou et al. 2021
KRN	MQTL_KRN_28			5	5.04	392.06	pza02040	magi62442	176,186,882	177,531,199		Zhou et al. 2021
KRN	MQTL_KRN_29			5	5.05	408.87	TIDP9188	umc1155	179,681,601	184,662,295		Zhou et al. 2021
KRN	MQTL_KRN_34			8	8.05	360.74	TIDP4634	IDP7284	133,392,120	137,533,473		Zhou et al. 2021
CF	qCF1-F2	B73xYi16	F2	1	1.02	92.97	umc1568	umc1976	16,037,234	21,883,821		Mei et 2020
CF	qCF1-BB	B73xYi16	F2:3	1	1.02	90.63	umc1568	umc1976	16,037,234	21,883,821		Mei et 2020
CF	qCF1-HC	B73xYi16	F2:3	1	1.02	90.63	umc1568	umc1976	16,037,234	21,883,821		Mei et 2020

CF	qCF4c-F2	B73xYi16	F2	4	4.09-4.10	317.68	umc1573	umc1532	240,523,216	242,207,541	Mei et 2020
CF	qCF4a-F2	B73xYi16	F2	4	4.09	269.25	umc1940	umc1631	224,941,231	235,760,235	Mei et 2020
CF	qCF4-BB	B73xYi16	F2:3	4	4.09	269.83	umc1940	umc1631	224,941,231	235,760,235	Mei et 2020
CF	qCF4-HC	B73xYi16	F2:3	4	4.09	270.5	umc1940	umc1631	224,941,231	235,760,235	Mei et 2020
CF	qCF4b-F2	B73xYi16	F2	4	4.08	198.82	umc2401	umc1051	189,872,212	196,014,456	Mei et 2020
CF	qCF7-BB	B73xYi16	F2:3	7	7.02	93.87	umc2092	umc1881	118,041,132	130,260,847	Mei et 2020
CF	qCF7-HC	B73xYi16	F2:3	7	7.02	93.87	umc2092	umc1881	118,041,132	130,260,847	Mei et 2020
EF	qEF1-BB	B73xYi16	F2:3	1	1.02	70.45	umc1685	bnlg1178	10,614,579	14,057,843	Mei et 2020
EF	qEF3-HC	B73xYi16	F2:3	3	3.04	111	umc1087	umc1223	27,840,060	56,948,312	Mei et 2020
EF	qEF4-BB	B73xYi16	F2:3	4	4.09	267.8	umc1940	umc1631	224,941,231	235,760,235	Mei et 2020
EF	qEF4-HC	B73xYi16	F2:3	4	4.09	268.83	umc1940	umc1631	224,941,231	235,760,235	Mei et 2020
EF	qEF7-BB	B73xYi16	F2:3	7	7.03	119.63	bnlg339	umc1301	132,218,974	160,923,525	Mei et 2020
EF	qEF7-HC	B73xYi16	F2:3	7	7.02-7.03	97.87	umc1881	umc1713	130,260,847	133,908,130	Mei et 2020
KRN	qKRN1-F2	B73xYi16	F2	1	1.07	263.33	phi037	umc1147	231,931,416	228,759,565	Mei et 2020
KRN	qKRN1b-BB	B73xYi16	F2:3	1	1.06	216.89	umc1321	umc2560	166,811,332	195,518,367	Mei et 2020

KRN	qKRN1a-BB	B73xYi16	F2:3	1	1.02	85.63	umc1568	umc1976	16,037,234	21,883,821		Mei et 2020
KRN	qKRN7-HC	B73xYi16	F2:3	7	7.02	92.87	umc2092	umc1881	118,041,132	130,260,847		Mei et 2020
FAS	fa_c1	PB260 x PB266	F2:3	7	7.03-7.04	86.57	umc1134	E41-M60-0289	132947391	173,807,744		Mendes-Moreira et al 2015
FAS	fa_c2	PB260 x PB266	F2:3	2	2.04	81.19	umc2030	E36-M50-0301	29562998	74,065,459		Mendes-Moreira et al 2015
FAS	fa_m1	PB260 x PB266	F2:3	7	7.03-7.04	87.57	umc1134	E41-M60-0289	132947391	173,807,744		Mendes-Moreira et al 2015
KRN	r2_m2	PB260 x PB266	F2:3	1	1.07	89.57	E36-M62-0063	umc1128	198,885,440	228,464,359		Mendes-Moreira et al 2015
KRN	qkrn7	Ye478 x Dan340	F2:3	7	7.03	72.51	bnlg339	umc1865	132,218,974	152,379,941		Lu et al 2010
EB	EB7.1		TeoNAM	7	7.02-7.03	64.8			103,900,000	132,700,000	121,500,000	Chen et al 2019
EB	EB7.1		TeoNAM	7	7.02-7.03	64.8			103,900,000	132,700,000	121,500,000	Chen et al 2019
KRN	KRN1.3		TeoNAM	1	1.11-1.12	165.7			298,100,000	299,600,000	298,500,000	Chen et al 2019
KRN	KRN4.3		TeoNAM	4	4.10	145.6			241,600,000	244,800,000	243,500,000	Chen et al 2019

KRN	KRN5.1	TeoNAM	5	5.00	12.7	2,300,000	2,900,000	2,400,000	Chen et al 2019
KRN	KRN7.1	TeoNAM	7	7.02	58.6	21,500,000	123,700,000	95,200,000	Chen et al 2019
KRN	KRN8.2	TeoNAM	8	8.07	106.8	169,600,000	173,400,000	171,300,000	Chen et al 2019
ERN		NAM	1	1.00	33.1			16,530,728	Brown et al 2011
ERN		NAM	1	1.02	43.2			26,283,010	Brown et al 2011
ERN		NAM	1	1.04	69.1			54,049,352	Brown et al 2011
ERN		NAM	1	1.07	116.5			204,199,175	Brown et al 2011
ERN		NAM	1	1.09	157.6			262,339,688	Brown et al 2011
ERN		NAM	1	1.11	198			294,904,517	Brown et al 2011
ERN		NAM	2	2.01	47.7			17,995,662	Brown et al 2011
ERN		NAM	2	2.04	70.9			48,526,009	Brown et al 2011
ERN		NAM	2	2.08	115.3			206,554,810	Brown et al 2011
ERN		NAM	2	2.09	141.3			226,450,732	Brown et al 2011
ERN		NAM	3	3.05	74.3			161,515,805	Brown et al 2011
ERN		NAM	3	3.07	111.2			203,318,354	Brown et al 2011
ERN		NAM	3	3.09	131.4			216,027,870	Brown et al 2011

ERN	NAM	4	4.01	12.2	3,547,577	Brown et al 2011
ERN	NAM	4	4.05	55.2	49,713,730	Brown et al 2011
ERN	NAM	4	4.08	107.9	204,764,641	Brown et al 2011
ERN	NAM	4	4.11	126.9	241,723,585	Brown et al 2011
ERN	NAM	5	5.00	25.4	6,820,446	Brown et al 2011
ERN	NAM	5	5.01	64.4	65,741,898	Brown et al 2011
ERN	NAM	5	5.04	79.7	167,875,726	Brown et al 2011
ERN	NAM	5	5.08	138	211,884,392	Brown et al 2011
ERN	NAM	6	6.00	10.7	77,189,686	Brown et al 2011
ERN	NAM	6	6.06	70.4	154,495,275	Brown et al 2011
ERN	NAM	7	7.00	45.8	22,002,484	Brown et al 2011
ERN	NAM	7	7.01	61.4	121,400,796	Brown et al 2011
ERN	NAM	7	7.01	71.2	131,103,742	Brown et al 2011
ERN	NAM	7	7.04	114.6	162,945,464	Brown et al 2011
ERN	NAM	8	8.02	42	18,466,260	Brown et al 2011
ERN	NAM	8	8.07	103.7	165,809,693	Brown et al 2011

ERN			NAM	9	9.01	0					3,955,834	Brown et al 2011
ERN			NAM	9	9.03	45.9					73,251,636	Brown et al 2011
ERN			NAM	9	9.05	74.2					136,597,896	Brown et al 2011
ERN			NAM	9	9.06	87.9					142,270,917	Brown et al 2011
ERN			NAM	10	10.03	36.2					45,411,991	Brown et al 2011
ERN			NAM	10	10.05	52.2					129,730,798	Brown et al 2011
ERN			NAM	10	10.05	64.5					137,132,509	Brown et al 2011
KRN	qKRN1b	Zong3 x K67-20	BC2RIL	1	1.10	275.34-275.43	PZE-101226279	PZE-101226356	281,249,878	281,336,729	281,249,878	Liu et al 2019
KRN	qKRN2a	Zong3 x K67-20	BC2RIL	2	2.01	31.04-39.27	SYN19564	PZE-102060571	32,086,898	40,380,450	32,086,898	Liu et al 2019
KRN	qKRN2b	Zong3 x K67-20	BC2RIL	2	2.07-2.08	175.05-187.23	SYN33465	PZA02890.4	183,364,359	195,895,088	183,364,359	Liu et al 2019
KRN	qKRN3.2a	Zong3 x K67-20	BC2RIL	3	3.05	136.13-138.06	PZE-103084544	PZE-103085749	140,629,342	142,701,212	140,629,342	Liu et al 2019
KRN	qKRN3.3a	Zong3 x K67-20	BC2RIL	3	3.07	193.06-193.83	PZE-103138441	PZE-103139252	197,777,734	198,592,431	197,777,734	Liu et al 2019

KRN	qKRN6.2c	Zong3 x K67-20	BC2RIL	6	6.01	34.29-57.64	PZE-106017625	PZE-106023672	43,454,942	60,136,153	43,454,942	Liu et al 2019
KRN	qKRN7b	Zong3 x K67-20	BC2RIL	7	7.03	139.58-140.17	SYN35523	PZE-107090737	150,084,073	150,667,116	150,084,073	Liu et al 2019

Supp Table 5. Information on QTL for prolificacy from literature

Trait	**QTL name**	**Original cross or population**	**population type**	**Chr.**	**BIN**	**Genetic Pos**	**Left marker**	**Right marker**	**Left position**	**Right position**	**Peak position**	**Ref.**
PROL	*prol1.1*	W22 x CIMMYT accession 8759	BC2S3 RIL	1	1.02				22,958,575	23,748,575		Wills et al 2013
PROL	*prol1.2*	W22 x CIMMYT accession 8759	BC2S3 RIL	1	1.06				181,909,234	182,289,234		Wills et al 2013
PROL	*prol1.3*	W22 x CIMMYT accession 8759	BC2S3 RIL	1	1.06				184,085,035	204,465,035		Wills et al 2013
PROL	*prol2.1*	W22 x CIMMYT accession 8759	BC2S3 RIL	2	2.04				46,043,276	64,773,276		Wills et al 2013
PROL	*prol3.1*	W22 x CIMMYT accession 8759	BC2S3 RIL	3	3.07				198,974,389	200,284,389		Wills et al 2013

PROL	*prol4.1*	W22 x CIMMYT accession 8759	BC2S3 RIL	4	4.06				161,087,836	169,167,836		Wills et al 2013
PROL	*prol4.2*	W22 x CIMMYT accession 8759	BC2S3 RIL	4	4.08				200,165,542	204,945,542		Wills et al 2013
PROL	*prol5.1*	W22 x CIMMYT accession 8759	BC2S3 RIL	5	5.04				143,449,564	148,699,564		Wills et al 2013
PROL	*Prol1*	IG-1 x BR-106	F2:3	2	2.03	54.9	umc1845	bnlg0166	15,447,080	29,201,899		Sabadin et al 2008
PROL	*Prol2*	IG-1 x BR-106	F2:3	7	7.04	122.2	dupssr13	umc1154	171,259,594	177,583,056		Sabadin et al 2008
PROL	*Prol3*	IG-1 x BR-106	F2:3	8	8.05	78.7	bnlg1176	bnlg1607	125,575,872	166,199,031		Sabadin et al 2008
PROL		A679 x S3	F3	1	1.09		phi055	phi055	254,190,642	271,963,644		DeLeon 2005
PROL		A679 x S3	F3	9	9.06		umc1366	umc1366	139,128,405	150,999,079		DeLeon 2005
PROL		A679 x S3	F3	6	6.01		bnlg426	bnlg426	8,694,567	87,364,434		DeLeon 2005
TILN	*TILN3.2*		TeoNAM	3	3.05	80.5			137,600,000	158,600,000	138,300,000	Chen et al 2019
TILN	*TILN5.1*		TeoNAM	5	5.03-5.04	75.4			36,000,000	140,700,000	69,000,000	Chen et al 2019
TILN	*TILN10.1*		TeoNAM	10	10.03	47.7			25,300,000	82,100,000	62,500,000	Chen et al 2019
PROL	*PROL1.1*		TeoNAM	1	1.02	41.1			23,600,000	24,700,000	23,600,000	Chen et al 2019
PROL	*PROL2.1*		TeoNAM	2	2.02	28.7			6,000,000	12,000,000	9,100,000	Chen et al 2019

PROL	*PROL3.1*		TeoNAM	3	3.08-3.09	140.4			212,600,000	220,600,000	218,500,000	Chen et al 2019
PROL	*PROL5.1*		TeoNAM	5	5.03	68			20,200,000	55,200,000	31,700,000	Chen et al 2019
EN	*qEN1*	Zong3 x K67-20	BC2RIL	1	1.01	9.42-27.5	SYN14142	PZE-101040601	9,488,662	27,588,230	9,488,662	Liu et al 2019
EN	*qEN3.1a*	Zong3 x K67-20	BC2RIL	3	3.03-3.04	125.45-129.49	PZE-103078226	SYN7602	129,683,521	133,865,336	129,683,521	Liu et al 2019
EN	*qEN3.2a*	Zong3 x K67-20	BC2RIL	3	3.05	137.52-137.52	PZE-103085353	PZE-103085353	142,154,401	142,154,401	142,154,401	Liu et al 2019
EN	*qEN3.8a*	Zong3 x K67-20	BC2RIL	3	3.06-3.07	186.79-192.56	PZE-103132640	PZE-103137887	191,431,510	197,314,312	191,431,510	Liu et al 2019
EN	*qEN5.3a*	Zong3 x K67-20	BC2RIL	5	5.04	137.93-138.07	PZE-105094633	PZE-105094725	142,021,233	142,160,004	142,021,233	Liu et al 2019
EN	*qEN5.4a*	Zong3 x K67-20	BC2RIL	5	5.05	179.62-183.68	SYN23388	PZE-105127547	184,890,420	189,130,768	184,890,420	Liu et al 2019
EN	*qEN8a*	Zong3 x K67-20	BC2RIL	8	8.03	102.38-102.38	PZE-108058030	PZE-108058030	105,776,099	105,776,099	105,776,099	Liu et al 2019

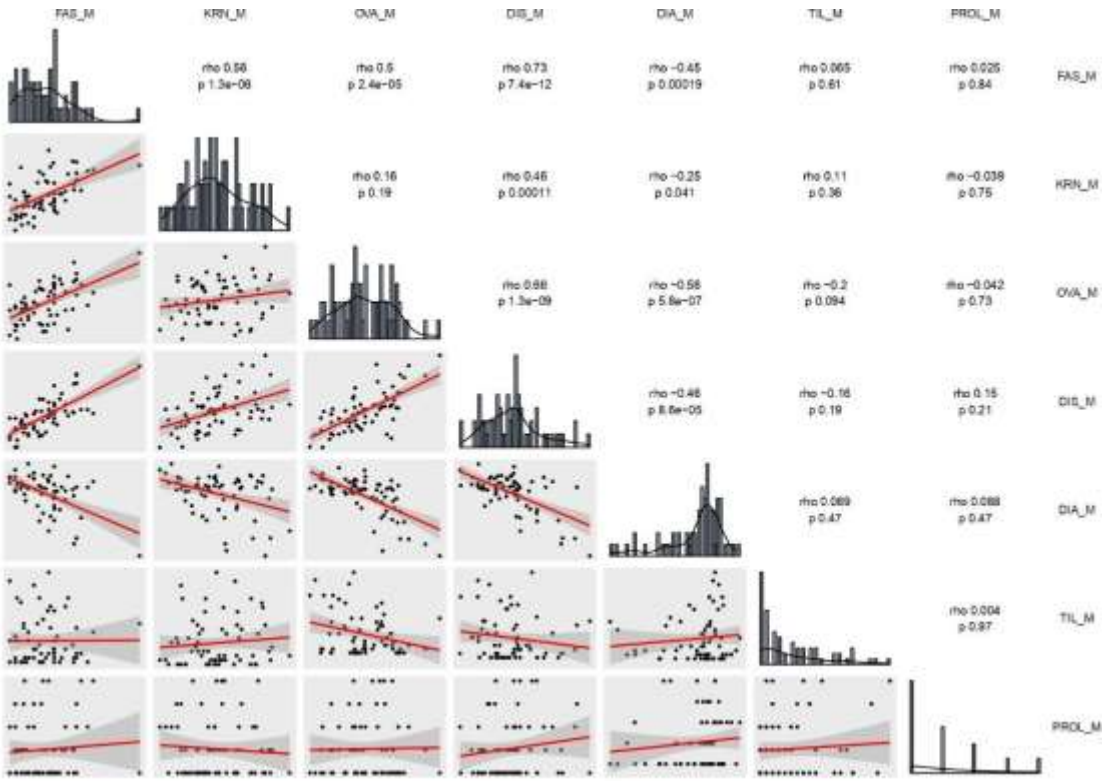

Supplementary Figure 1. Distribution frequency histograms of, and correlation (Spearman) among all traits estimated on the B×L.

The upper right part presents all correlation indexes (*rho*, thus the upper number) and corresponding significant levels (*p*, thus the lower number). Minus rho values show negative correlation between two traits, and vice versa. The lower left part presents scatter plots and fitter curve (the red line inside) between two traits. The diagonal shows histogram charts of each trait. DIA (ear diameters rate), DIS (kernel row disorder), OVA (ear ovality), FAS (ear fasciation index), KRN (kernel row number), PROL (prolificacy), TIL (number of tillers), M, mean value.

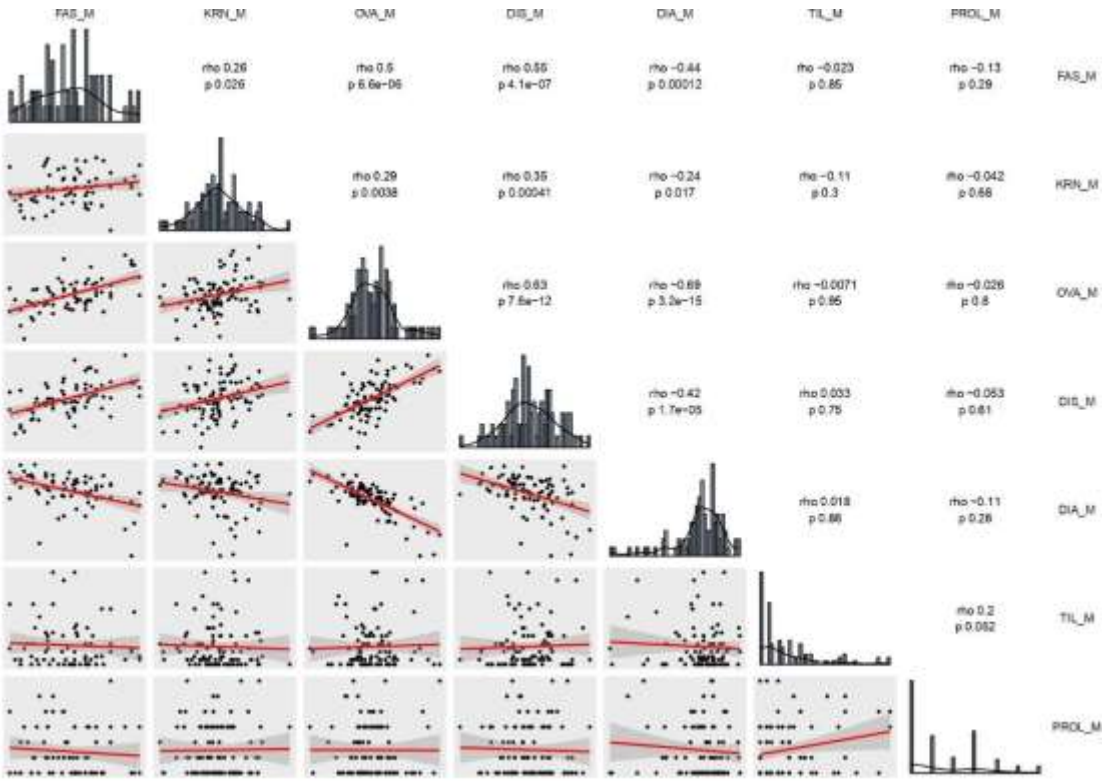

Supplementary Figure 2. Distribution frequency histograms of, and correlation (Spearman) among all traits estimated on the L×L.

The upper right part presents all correlation indexes (*rho*, thus the upper number) and corresponding significant levels (*p*, thus the lower number). Minus rho values show negative correlation between two traits, and vice versa. The lower left part presents scatter plots and fitter curve (the red line inside) between two traits. The diagonal shows histogram charts of each trait. DIA (ear diameters rate), DIS (kernel row disorder), OVA (ear ovality), FAS (ear fasciation index), KRN (kernel row number), PROL (prolificacy), TIL (number of tillers), M, mean value.

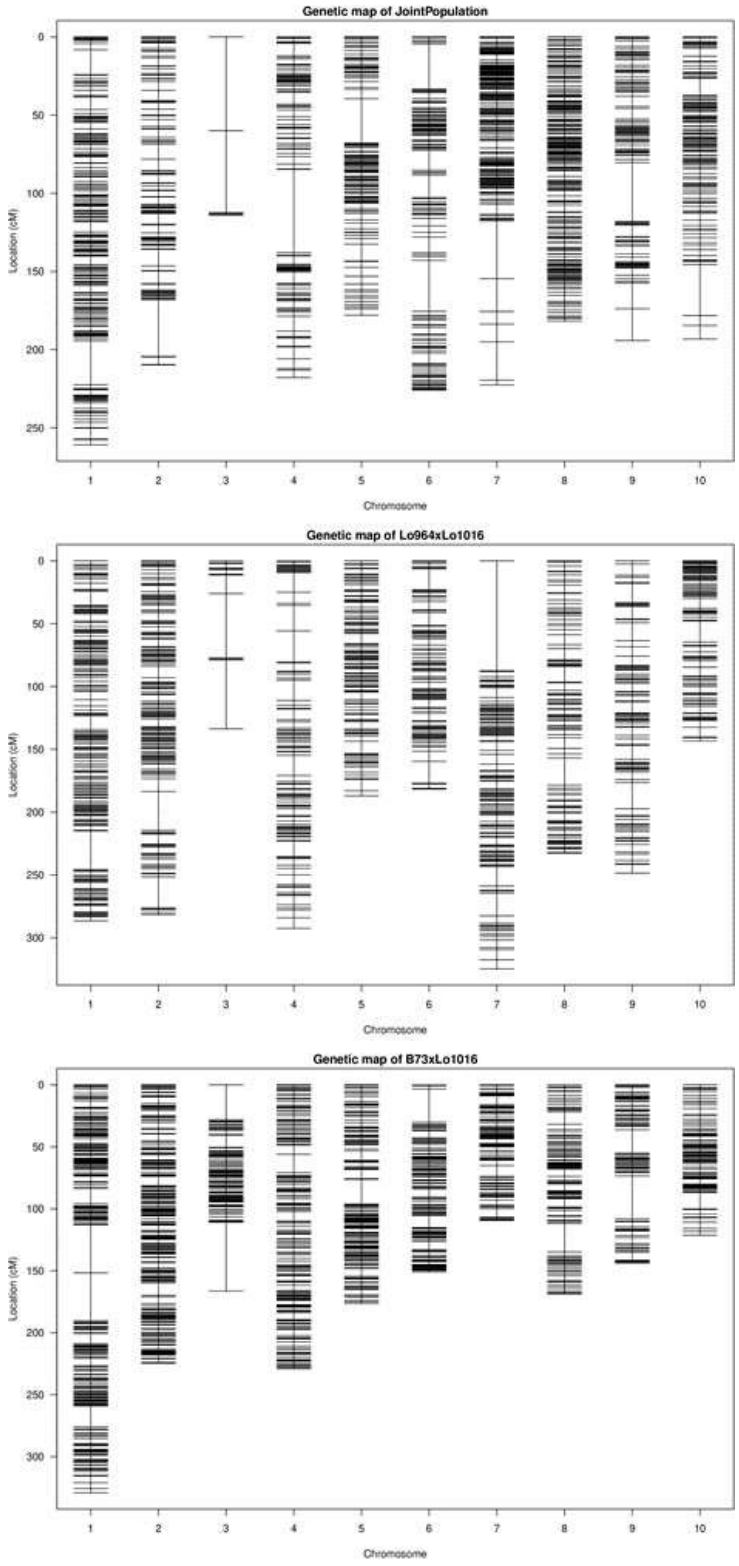

Supplementary Figure 3. Linkage map plot. From top to bottom: JP, L×L, B×L

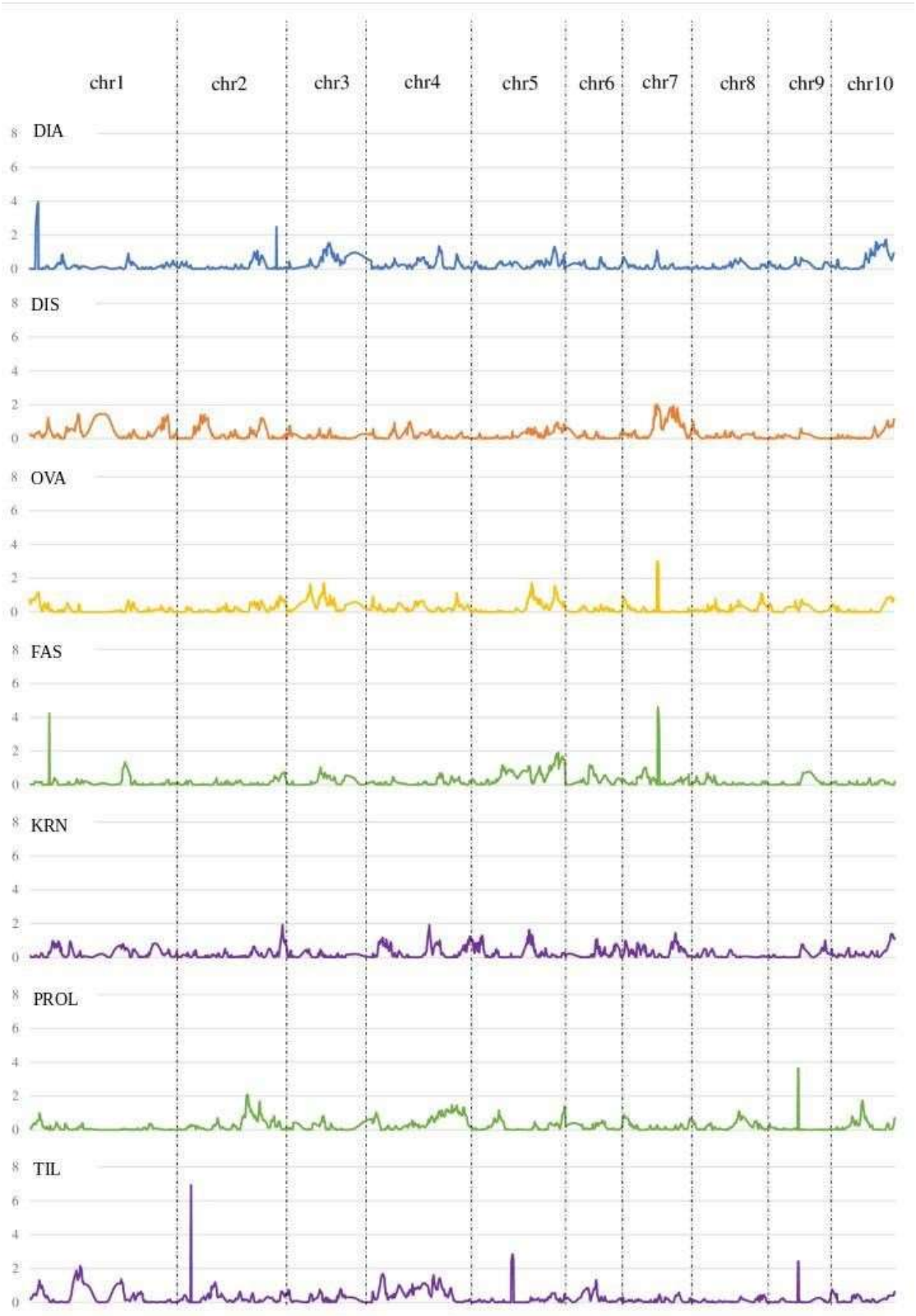

Supplementary Figure 4. QTL LOD profiles obtained by B×L, for DIA (ear diameters rate), DIS (kernel row disorder), OVA (ear ovality), FAS (ear fasciation index), KRN (kernel row number), PROL (prolificacy), TIL (number of tillers).

Supplementary Figure 5. QTL LOD profiles obtained by L×L, for DIA (ear diameters rate), DIS (kernel row disorder), OVA (ear ovality), FAS (ear fasciation index), KRN (kernel row number), PROL (prolificacy), TIL (number of tillers).

A

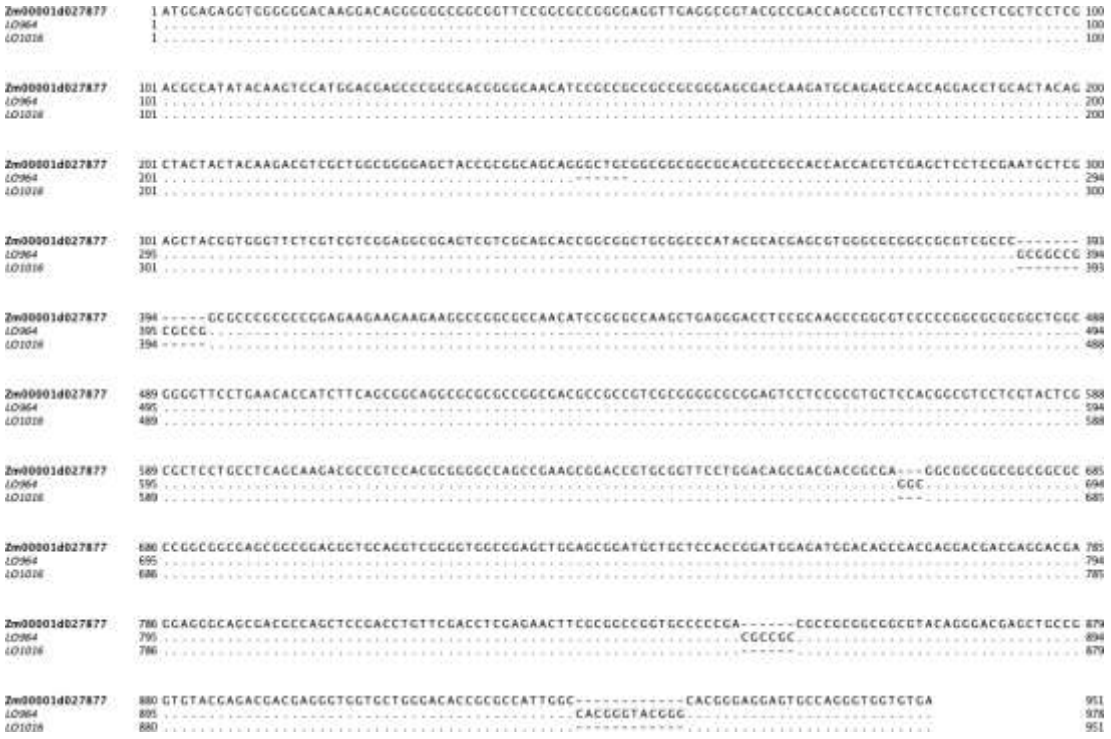

B

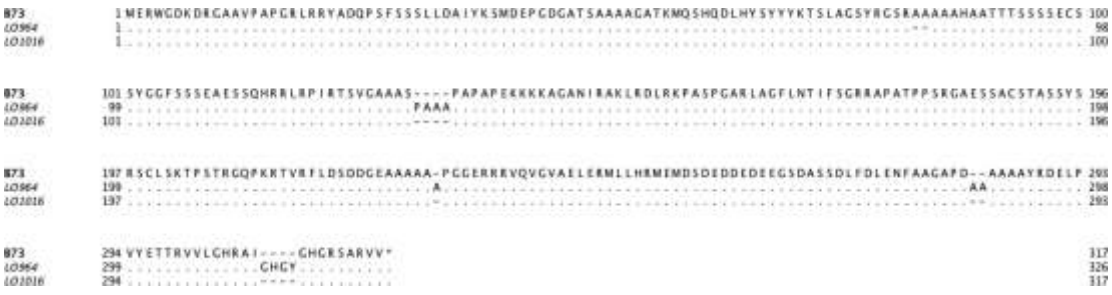

Supplementary Figure 6. Multialignment of *Bgh1* alleles. Alignment of nucleotides of the coding sequence A) and of the corresponding amino acids B) from LO964 and LO1016 to the reference sequence B73 version 4.

A

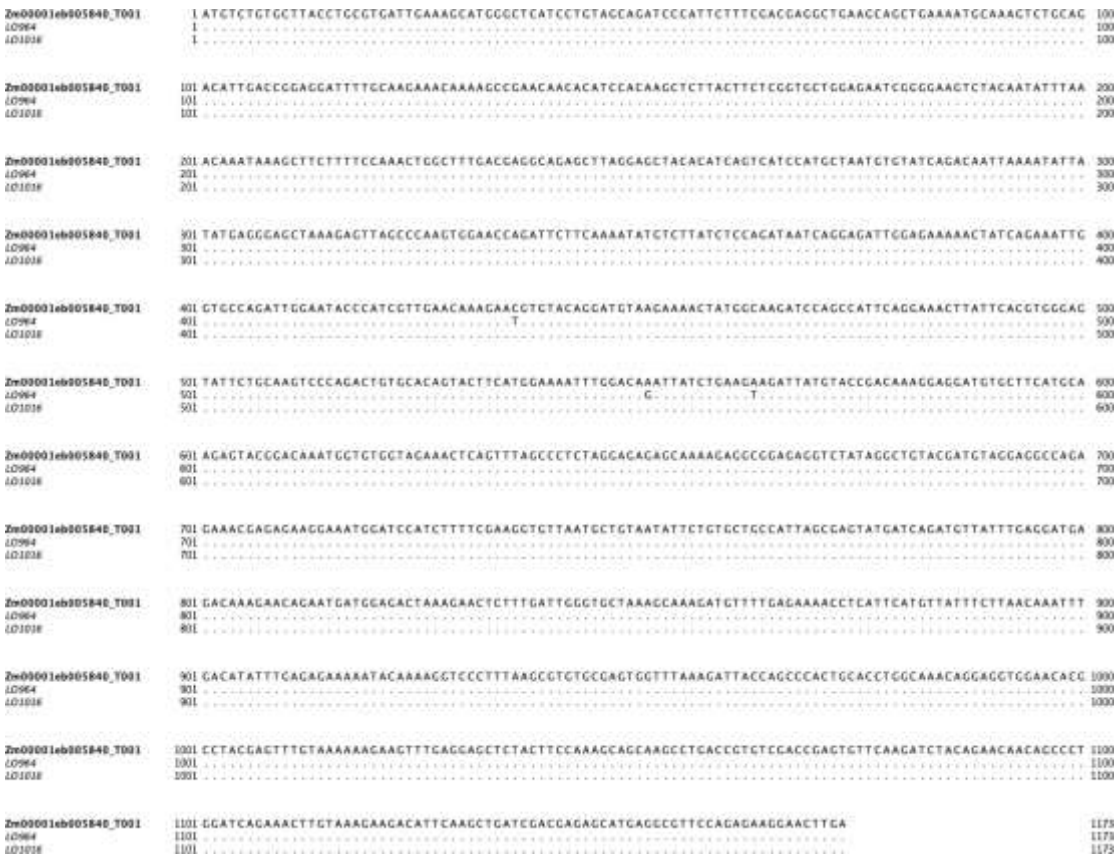

B

Supplementary Figure 7. Multialignment of *ct2* alleles. Alignment of nucleotides of the coding sequence A) and of the corresponding amino acids B) from LO964 and LO1016 to the reference sequence B73 version 4

A

B

Supplementary Figure 8. Multialignment of *ra1* alleles. Alignment of nucleotides of the coding sequence A) and of the corresponding amino acids B) from LO964 and LO1016 to the reference sequence B73 version 4

A

B

Supplementary Figure 9. Multialignment of *bif1* alleles. Alignment of nucleotides of the coding sequence A) and of the corresponding amino acids B) from LO964 and LO1016 to the reference sequence B73 version 4

A

B

Supplementary Figure 10. Multialignment of *crr1* alleles. Alignment of nucleotides of the coding sequence A) and of the corresponding amino acids B) from LO964 and LO1016 to the reference sequence B73 version 4

Reference

Abendroth, L.J., Elmore, R.W., Boyer, M.J., and Marlay, S.K. (2011) *Corn Growth and Development*, Ames, IA: Iowa State University Extension.

Agarwal, A., Yadava, P., Kumar, K., Singh, I., Kaul, T., Pattanayak, A. and Agrawal, P.K. (2018) Insights into maize genome editing via CRISPR/Cas9. *Physiol. Mol. Biol. Plants*, **24**, 175–183. Available at: http://dx.doi.org/10.1007/s12298-017-0502-3.

Alessia Losa, Hans Hartings, Alberto Verderio, Mario Motto (2011) Assesment of genetic diversity and relationships among maize inbred lines developed in Italy. *Maydica*, **56**.

Bandillo, N., Raghavan, C., Muyco, P.A., et al. (2013) Multi-parent advanced generation inter-cross (MAGIC) populations in rice: progress and potential for genetics research and breeding. *Rice (N. Y.)*, **6**, 11. Available at: http://dx.doi.org/10.1186/1939-8433-6-11.

Barazesh, S. and McSteen, P. (2008) Barren inflorescence1 functions in organogenesis during vegetative and inflorescence development in maize. *Genetics*, **179**, 389–401. Available at: http://dx.doi.org/10.1534/genetics.107.084079.

Bommert, P., Je, B.I., Goldshmidt, A. and Jackson, D. (2013) The maize Gα gene COMPACT PLANT2 functions in CLAVATA signalling to control shoot meristem size. *Nature*, **502**, 555–558. Available at: http://dx.doi.org/10.1038/nature12583.

Bommert, P., Nagasawa, N.S. and Jackson, D. (2013) Quantitative variation in maize kernel row number is controlled by the FASCIATED EAR2 locus. *Nat. Genet.*, **45**, 334–337. Available at: http://dx.doi.org/10.1038/ng.2534.

Brand, U., Fletcher, J.C., Hobe, M., Meyerowitz, E.M. and Simon, R. (2000) Dependence of stem cell fate in Arabidopsis on a feedback loop regulated by CLV3 activity. *Science*, **289**, 617–619. Available at: http://dx.doi.org/10.1126/science.289.5479.617.

Brown, P.J., Upadyayula, N., Mahone, G.S., et al. (2011) Distinct genetic architectures for male and female inflorescence traits of maize. *PLoS Genet.*, **7**, e1002383. Available at: http://dx.doi.org/10.1371/journal.pgen.1002383.

Chen, Q., Yang, C.J., York, A.M., et al. (2019a) TeoNAM: a nested association mapping population for domestication and agronomic trait analysis in maize. *bioRxiv*. Available at: http://dx.doi.org/10.1101/647461.

Chen, Q., Yang, C.J., York, A.M., et al. (2019b) TeoNAM: A nested association mapping population for domestication and agronomic trait analysis in maize. *Genetics*, **213**, 1065–1078. Available at: http://dx.doi.org/10.1534/genetics.119.302594.

Chen, W., Chen, L., Zhang, X., et al. (2022) Convergent selection of a WD40 protein that enhances grain yield in maize and rice. *Science*, **375**, eabg7985. Available at: http://dx.doi.org/10.1126/science.abg7985.

Choudhary, M., Wani, S.H., Kumar, P., Bagaria, P.K., Rakshit, S., Roorkiwal, M. and Varshney, R.K. (2019) QTLian breeding for climate resilience in cereals: progress and prospects. *Funct. Integr. Genomics*, **19**, 685–701. Available at: http://dx.doi.org/10.1007/s10142-019-00684-1.

Chu, H., Qian, Q., Liang, W., et al. (2006) The floral organ number4 gene encoding a putative ortholog of Arabidopsis CLAVATA3 regulates apical meristem size in rice. *Plant Physiol.*, **142**, 1039–1052. Available at: http://dx.doi.org/10.1104/pp.106.086736.

Cingolani, P., Platts, A., Wang, L.L., Coon, M., Nguyen, T., Wang, L., Land, S.J., Lu, X. and Ruden, D.M. (2012) A program for annotating and predicting the effects of single nucleotide polymorphisms, SnpEff: SNPs in the genome of Drosophila melanogaster strain w1118; iso-2; iso-3. *Fly (Austin)*, **6**, 80–92. Available at: http://dx.doi.org/10.4161/fly.19695.

Clark, S.E., Running, M.P. and Meyerowitz, E.M. (1993) CLAVATA1, a regulator of meristem and flower development in Arabidopsis. *Development*, **119**, 397–418. Available at: https://www.ncbi.nlm.nih.gov/pubmed/8287795.

Dempewolf, H. (2010) Getting domestication straight: ramosa1 in maize. *Mol. Ecol.*, **19**, 1267–1269. Available at: http://dx.doi.org/10.1111/j.1365-294X.2010.04563.x.

Doebley, J., Stec, A. and Gustus, C. (1995) Teosinte branched1 and the origin of maize: Evidence for epistasis and the evolution of dominance. *Genetics*, **141**, 333–346. Available at: http://dx.doi.org/10.1093/genetics/141.1.333.

Domagalska, M.A. and Leyser, O. (2011) Signal integration in the control of shoot branching. *Nat. Rev. Mol. Cell Biol.*, **12**, 211–221. Available at: http://dx.doi.org/10.1038/nrm3088.

Dong, Z., Li, W., Unger-Wallace, E., Yang, J., Vollbrecht, E. and Chuck, G. (2017) Ideal crop plant architecture is mediated by tassels replace upper ears1, a BTB/POZ ankyrin repeat gene directly targeted by TEOSINTE BRANCHED1. *Proc. Natl. Acad. Sci. U. S. A.*, **114**, E8656–E8664. Available at: http://dx.doi.org/10.1073/pnas.1714960114.

Du, Y., Liu, L., Li, M., Fang, S., Shen, X., Chu, J. and Zhang, Z. (2017) UNBRANCHED3 regulates branching by modulating cytokinin biosynthesis and signaling in maize and rice. *New Phytol.*, **214**, 721–733. Available at: http://dx.doi.org/10.1111/nph.14391.

Du, Y., Liu, L., Peng, Y., Li, M., Li, Y., Liu, D., Li, X. and Zhang, Z. (2020) UNBRANCHED3 expression and inflorescence development is mediated by UNBRANCHED2 and the distal enhancer, KRN4, in maize. *PLoS Genet.*, **16**, e1008764. Available at: http://dx.doi.org/10.1371/journal.pgen.1008764.

Edgar, R.C. (2004) MUSCLE: a multiple sequence alignment method with reduced time and space complexity. *BMC Bioinformatics*, **5**, 113. Available at: http://dx.doi.org/10.1186/1471-2105-5-113.

Fan, C., Wu, Y., Yang, Q., Yang, Y., Meng, Q., Zhang, K., Li, J., Wang, J. and Zhou, Y. (2014) A novel single-nucleotide mutation in a CLAVATA3 gene homolog controls a multilocular silique trait in Brassica rapa L. *Mol. Plant*, **7**, 1788–1792. Available at: http://dx.doi.org/10.1093/mp/ssu090.

Gallavotti, A., Long, J.A., Stanfield, S., Yang, X., Jackson, D., Vollbrecht, E. and Schmidt, R.J. (2010) The control of axillary meristem fate in the maize ramosa pathway. *Development*, **137**, 2849–2856. Available at: http://dx.doi.org/10.1242/dev.051748.

Galli, M. and Gallavotti, A. (2016) Expanding the regulatory network for meristem size in plants. *Trends Genet.*, **32**, 372–383. Available at: http://dx.doi.org/10.1016/j.tig.2016.04.001.

Glover, K.D., Wang, D., Arelli, P.R., Carlson, S.R., Cianzio, S.R. and Diers, B.W. (2004) Near isogenic lines confirm a soybean cyst nematode resistance gene from PI 88788 on linkage group J. *Crop Sci.*, **44**, 1505–1505. Available at: http://dx.doi.org/10.2135/cropsci2004.1505a.

Huang, B.E., George, A.W., Forrest, K.L., Kilian, A., Hayden, M.J., Morell, M.K. and Cavanagh, C.R. (2012) A multiparent advanced generation inter-cross population for genetic analysis in wheat. *Plant Biotechnol. J.*, **10**, 826–839. Available at: http://dx.doi.org/10.1111/j.1467-7652.2012.00702.x.

Hufford, M.B., Seetharam, A.S., Woodhouse, M.R., et al. (2021) De novo assembly, annotation, and comparative analysis of 26 diverse maize genomes. *Science*, **373**, 655–662. Available at: http://dx.doi.org/10.1126/science.abg5289.

Iliev, I. and Kitin, P. (2011) Origin, morphology, and anatomy of fasciation in plants cultured in vivo and in vitro. *Plant Growth Regul.*, **63**, 115–129. Available at: http://dx.doi.org/10.1007/s10725-010-9540-3.

Jaganathan, D., Bohra, A., Thudi, M. and Varshney, R.K. (2020) Fine mapping and gene cloning in the post-NGS era: advances and prospects. *Züchter Genet. Breed. Res.* , **133**, 1791–1810. Available at: http://dx.doi.org/10.1007/s00122-020-03560-w.

Je, B.I., Gruel, J., Lee, Y.K., et al. (2016) Signaling from maize organ primordia via FASCIATED EAR3 regulates stem cell proliferation and yield traits. *Nat. Genet.*, **48**, 785–791. Available at: http://dx.doi.org/10.1038/ng.3567.

Je, B.I., Xu, F., Wu, Q., et al. (2018) The CLAVATA receptor FASCIATED EAR2 responds to distinct CLE peptides by signaling through two downstream effectors. *Elife*, **7**. Available at: http://dx.doi.org/10.7554/elife.35673.

Jewiss, O.R. (1972) Tillering in grasses-its significance and control. *Grass Forage Sci.*, **27**, 65–82. Available at: http://dx.doi.org/10.1111/j.1365-2494.1972.tb00689.x.

Kim, D.E., Jeong, J.-H., Kang, Y.M., et al. (2022) The impact of fasciation on maize inflorescence architecture. *J. Plant Biol.*, **65**, 87–98. Available at: http://dx.doi.org/10.1007/s12374-021-09342-1.

Kumar, S., Stecher, G., Li, M., Knyaz, C. and Tamura, K. (2018) MEGA X: Molecular evolutionary genetics analysis across computing platforms. *Mol. Biol. Evol.*, **35**, 1547–1549. Available at: http://dx.doi.org/10.1093/molbev/msy096.

Kyozuka, J., Tokunaga, H. and Yoshida, A. (2014) Control of grass inflorescence form by the fine-tuning of meristem phase change. *Curr. Opin. Plant Biol.*, **17**, 110–115. Available at: http://dx.doi.org/10.1016/j.pbi.2013.11.010.

Li, H. (2011) A statistical framework for SNP calling, mutation discovery, association mapping and population genetical parameter estimation from sequencing data. *Bioinformatics*, **27**, 2987–2993. Available at: http://dx.doi.org/10.1093/bioinformatics/btr509.

Li, H. and Durbin, R. (2009) Fast and accurate short read alignment with Burrows-Wheeler transform. *Bioinformatics*, **25**, 1754–1760. Available at: http://dx.doi.org/10.1093/bioinformatics/btp324.

Li, X., Qian, Q., Fu, Z., et al. (2003) Control of tillering in rice. *Nature*, **422**, 618–621. Available at: http://dx.doi.org/10.1038/nature01518.

Liu, L., Du, Y., Huo, D., et al. (2015) Genetic architecture of maize kernel row number and whole genome prediction. *Züchter Genet. Breed. Res.* , **128**, 2243–2254. Available at: http://dx.doi.org/10.1007/s00122-015-2581-2.

Liu, L., Du, Y., Shen, X., et al. (2015) KRN4 controls quantitative variation in maize kernel row number. *PLoS Genet.*, **11**, e1005670. Available at: http://dx.doi.org/10.1371/journal.pgen.1005670.

Liu, L., Tong, H., Xiao, Y., et al. (2015) Activation of Big Grain1 significantly improves grain size by regulating auxin transport in rice. *Proc. Natl. Acad. Sci. U. S. A.*, **112**, 11102–11107. Available at: http://dx.doi.org/10.1073/pnas.1512748112.

Liu, X., Galli, M., Camehl, I. and Gallavotti, A. (2019) RAMOSA1 ENHANCER LOCUS2-mediated transcriptional repression regulates vegetative and reproductive architecture. *Plant Physiol.*, **179**, 348–363. Available at: http://dx.doi.org/10.1104/pp.18.00913.

Mackay, I.J., Bansept-Basler, P., Barber, T., et al. (2014) An eight-parent multiparent advanced generation inter-cross population for winter-sown wheat: creation, properties, and validation. *G3 (Bethesda)*, **4**, 1603–1610. Available at: http://dx.doi.org/10.1534/g3.114.012963.

Maluszynski, M., Kasha, K. and Forster, B.P. eds. (2014) *Doubled haploid production in crop plants*, New York, NY: Springer.

McMullen, M.D., Kresovich, S., Villeda, H.S., et al. (2009) Genetic properties of the maize nested association mapping population. *Science*, **325**, 737–740. Available at: http://dx.doi.org/10.1126/science.1174320.

Mei, X., Dong, E., Liang, Q., Bai, Y., Nan, J., Yang, Y. and Cai, Y. (2021) Identification of QTL for fasciated ear related traits in maize. *Crop Sci.*, **61**, 1184–1193. Available at: http://dx.doi.org/10.1002/csc2.20435.

Mendes-Moreira, P., Alves, M.L., Satovic, Z., Dos Santos, J.P., Santos, J.N., Souza, J.C., Pêgo, S.E., Hallauer, A.R. and Vaz Patto, M.C. (2015) Genetic architecture of ear fasciation in maize (Zea mays) under QTL scrutiny. *PLoS One*, **10**, e0124543. Available at: http://dx.doi.org/10.1371/journal.pone.0124543.

Meng, L., Guo, L., Ponce, K., Zhao, X. and Ye, G. (2016) Characterization of three Indica rice multiparent advanced generation intercross (MAGIC) populations for quantitative trait loci identification. *Plant Genome*, **9**, lantgenome2015.10.0109. Available at: http://dx.doi.org/10.3835/plantgenome2015.10.0109.

Meng, L., Li, H., Zhang, L. and Wang, J. (2015) QTL IciMapping: Integrated software for genetic linkage map construction and quantitative trait locus mapping in biparental populations. *Crop J.*, **3**, 269–283. Available at: http://dx.doi.org/10.1016/j.cj.2015.01.001.

Müller, R., Borghi, L., Kwiatkowska, D., Laufs, P. and Simon, R. (2006) Dynamic and compensatory responses of Arabidopsis shoot and floral meristems to CLV3 signaling. *Plant Cell*, **18**, 1188–1198. Available at: http://dx.doi.org/10.1105/tpc.105.040444.

Opsahl-Ferstad, H.G., Le Deunff, E., Dumas, C. and Rogowsky, P.M. (1997) ZmEsr, a novel endosperm-specific gene expressed in a restricted region around the maize embryo. *Plant J.*, **12**, 235–246. Available at: http://dx.doi.org/10.1046/j.1365-313x.1997.12010235.x.

Ortez, O.A., McMechan, A.J., Hoegemeyer, T., Ciampitti, I.A., Nielsen, R., Thomison, P.R. and Elmore, R.W. (2022) Abnormal ear development in corn: A review. *Agron. J.*, **114**, 1168–1183. Available at: http://dx.doi.org/10.1002/agj2.20986.

Otegui, M.E. and Bonhomme, R. (1998) Grain yield components in maize. *Field Crops Res.*, **56**, 247–256. Available at: http://dx.doi.org/10.1016/s0378-4290(97)00093-2.

Pascual, L., Desplat, N., Huang, B.E., et al. (2015) Potential of a tomato MAGIC population to decipher the genetic control of quantitative traits and detect causal variants in the resequencing era. *Plant Biotechnol. J.*, **13**, 565–577. Available at: http://dx.doi.org/10.1111/pbi.12282.

Pertea, G. and Pertea, M. (2020) GFF utilities: GffRead and GffCompare. *F1000Res.*, **9**, 304. Available at: http://dx.doi.org/10.12688/f1000research.23297.2.

Portwood, J.L., 2nd, Woodhouse, M.R., Cannon, E.K., et al. (2019) MaizeGDB 2018: the maize multi-genome genetics and genomics database. *Nucleic Acids Res.*, **47**, D1146–D1154. Available at: http://dx.doi.org/10.1093/nar/gky1046.

Prakash, N.R., Zunjare, R.U., Muthusamy, V., Chand, G., Kamboj, M.C., Bhat, J.S. and Hossain, F. (2019) Genetic analysis of prolificacy in "Sikkim Primitive"—A prolific maize (Zea mays) landrace of North-Eastern Himalaya. *Plant Breed.*, **138**, 781-789. Available at: http://dx.doi.org/10.1111/pbr.12736.

Rodriguez-Leal, D., Xu, C., Kwon, C.-T., et al. (2019) Evolution of buffering in a genetic circuit controlling plant stem cell proliferation. *Nat. Genet.*, **51**, 786–792. Available at: http://dx.doi.org/10.1038/s41588-019-0389-8.

Rotili, D.H., Abeledo, L.G., Martínez Larrea, S. and Maddonni, G.Á. (2022) Grain yield and kernel setting of multiple-shoot and/or multiple-ear maize hybrids. *Field Crops Res.*, **279**, 108471. Available at: http://dx.doi.org/10.1016/j.fcr.2022.108471.

Rousselle, Y., Jones, E., Charcosset, A., et al. (2015) Study on essential derivation in maize: III. Selection and evaluation of a panel of single nucleotide polymorphism loci for use in European and north American germplasm. *Crop Sci.*, **55**, 1170–1180. Available at: http://dx.doi.org/10.2135/cropsci2014.09.0627.

Salvi, S. and Tuberosa, R. (2005) To clone or not to clone plant QTLs: present and future challenges. *Trends Plant Sci.*, **10**, 297–304. Available at: http://dx.doi.org/10.1016/j.tplants.2005.04.008.

Schnable, P.S., Ware, D., Fulton, R.S., et al. (2009) The B73 maize genome: complexity, diversity, and dynamics. *Science*, **326**, 1112–1115. Available at: http://dx.doi.org/10.1126/science.1178534.

Schoof, H., Lenhard, M., Haecker, A., Mayer, K.F.X., Jürgens, G. and Laux, T. (2000) The stem cell population of Arabidopsis shoot meristems is maintained by a

regulatory loop between the CLAVATA and WUSCHEL genes. *Cell*, **100**, 635–644. Available at: http://dx.doi.org/10.1016/s0092-8674(00)80700-x.

Sigmon, B. and Vollbrecht, E. (2010) Evidence of selection at the ramosa1 locus during maize domestication. *Mol. Ecol.*, **19**, 1296–1311. Available at: http://dx.doi.org/10.1111/j.1365-294X.2010.04562.x.

Simmons, C.R., Weers, B.P., Reimann, K.S., Abbitt, S.E., Frank, M.J., Wang, W., Wu, J., Shen, B. and Habben, J.E. (2020) Maize BIG GRAIN1 homolog overexpression increases maize grain yield. *Plant Biotechnol. J.*, **18**, 2304–2315. Available at: http://dx.doi.org/10.1111/pbi.13392.

Sokal, R.R. and Rohlf, F.J. (2012) *Biometry* 4th ed., New York, NY: W.H. Freeman.

Somssich, M., Je, B.I., Simon, R. and Jackson, D. (2016) CLAVATA-WUSCHEL signaling in the shoot meristem. *Development*, **143**, 3238–3248. Available at: http://dx.doi.org/10.1242/dev.133645.

Stelpflug, S.C., Sekhon, R.S., Vaillancourt, B., Hirsch, C.N., Buell, C.R., Leon, N. and Kaeppler, S.M. (2016) An expanded maize gene expression atlas based on RNA sequencing and its use to explore root development. *Plant Genome*, **9**, lantgenome2015.04.0025. Available at: http://dx.doi.org/10.3835/plantgenome2015.04.0025.

Stitzer, M.C. and Ross-Ibarra, J. (2018) Maize domestication and gene interaction. *PeerJ*. Available at: http://dx.doi.org/10.7287/peerj.preprints.26502.

Suzaki, T., Sato, M., Ashikari, M., Miyoshi, M., Nagato, Y. and Hirano, H.-Y. (2004) The gene FLORAL ORGAN NUMBER1 regulates floral meristem size in rice and encodes a leucine-rich repeat receptor kinase orthologous to Arabidopsis CLAVATA1. *Development*, **131**, 5649–5657. Available at: http://dx.doi.org/10.1242/dev.01441.

Suzaki, T., Yoshida, A. and Hirano, H.-Y. (2008) Functional diversification of CLAVATA3-related CLE proteins in meristem maintenance in rice. *Plant Cell*, **20**, 2049–2058. Available at: http://dx.doi.org/10.1105/tpc.107.057257.

Tanksley, S.D. (2004) The genetic, developmental, and molecular bases of fruit size and shape variation in tomato. *Plant Cell*, **16 Suppl**, S181-9. Available at: http://dx.doi.org/10.1105/tpc.018119.

Trotochaud, A.E., Hao, T., Wu, G., Yang, Z. and Clark, S.E. (1999) The CLAVATA1 receptor-like kinase requires CLAVATA3 for its assembly into a signaling complex that includes KAPP and a Rho-related protein. *Plant Cell*, **11**, 393–406. Available at: http://dx.doi.org/10.1105/tpc.11.3.393.

Wang, Z., Gao, J., Li, Y., et al. (2021) Combined linkage analysis and Genome-wide association study reveal QTLs and candidate genes conferring genetic control of prolificacy trait in maize. *Preprints*. Available at: http://dx.doi.org/10.20944/preprints202101.0185.v1.

Waterhouse, A.M., Procter, J.B., Martin, D.M.A., Clamp, M. and Barton, G.J. (2009) Jalview Version 2--a multiple sequence alignment editor and analysis workbench. *Bioinformatics*, **25**, 1189–1191. Available at: http://dx.doi.org/10.1093/bioinformatics/btp033.

White, O.E. (1948) Fasciation. *Bot. Rev.*, **14**, 319–358. Available at: http://dx.doi.org/10.1007/bf02861723.

Wickham, H., Averick, M., Bryan, J., et al. (2019) Welcome to the tidyverse. *J. Open Source Softw.*, **4**, 1686. Available at: http://dx.doi.org/10.21105/joss.01686.

Wills, D.M., Whipple, C.J., Takuno, S., Kursel, L.E., Shannon, L.M., Ross-Ibarra, J. and Doebley, J.F. (2013) From many, one: genetic control of prolificacy during maize domestication. *PLoS Genet.*, **9**, e1003604. Available at: http://dx.doi.org/10.1371/journal.pgen.1003604.

Xu, M., Zhu, L., Shou, H. and Wu, P. (2005) A PIN1 family gene, OsPIN1, involved in auxin-dependent adventitious root emergence and tillering in rice. *Plant Cell Physiol.*, **46**, 1674–1681. Available at: http://dx.doi.org/10.1093/pcp/pci183.

Xu, Y. (2012) *Molecular Plant Breeding*, Wallingford, England: CABI Publishing.

Yang, C.J., Samayoa, L.F., Bradbury, P.J., et al. (2019) The genetic architecture of teosinte catalyzed and constrained maize domestication. *Proc. Natl. Acad. Sci. U. S. A.*, **116**, 5643–5652. Available at: http://dx.doi.org/10.1073/pnas.1820997116.

Yu, J., Holland, J.B., McMullen, M.D. and Buckler, E.S. (2008) Genetic design and statistical power of nested association mapping in maize. *Genetics*, **178**, 539–551. Available at: http://dx.doi.org/10.1534/genetics.107.074245.

Zhang, Y., Jiao, F., Li, J., Pei, Y., Zhao, M., Song, X. and Guo, X. (2022) Transcriptomic analysis of the maize inbred line Chang7-2 and a large-grain mutant tc19. *BMC Genomics*, **23**, 4. Available at: http://dx.doi.org/10.1186/s12864-021-08230-9.

Zhou, Y., Kusmec, A., Mirnezami, S.V., et al. (2021) Identification and utilization of genetic determinants of trait measurement errors in image-based, high-throughput phenotyping. *Plant Cell*, **33**, 2562–2582. Available at: http://dx.doi.org/10.1093/plcell/koab134.

Gallavotti, Andrea, Jeff A. Long, Sharon Stanfield, Xiang Yang, David Jackson, Erik Vollbrecht, and Robert J. Schmidt. 2010. “The Control of Axillary Meristem Fate in the Maize Ramosa Pathway.” *Development (Cambridge, England)* 137 (17): 2849–56.

Liu, Xue, Mary Galli, Iris Camehl, and Andrea Gallavotti. 2019. “RAMOSA1 ENHANCER LOCUS2-Mediated Transcriptional Repression Regulates Vegetative and Reproductive Architecture.” *Plant Physiology* 179 (1): 348–63.
Robertson, Donald S. 1985. “A Possible Technique for Isolating Genic DNA for Quantitative Traits in Plants.” *Journal of Theoretical Biology* 117 (1): 1–10.
Schnable, James C., and Michael Freeling. 2011. “Genes Identified by Visible Mutant Phenotypes Show Increased Bias toward One of Two Subgenomes of Maize.” *PloS One* 6 (3): e17855.
Tai, Huanhuan, Nina Opitz, Andrew Lithio, Xin Lu, Dan Nettleton, and Frank Hochholdinger. 2016. “Non-Syntenic Genes Drive RTCS-Dependent Regulation of the Embryo Transcriptome during Formation of Seminal Root Primordia in Maize (Zea MaysL.).” *Journal of Experimental Botany*, November, erw422.